FACULTY
OF INFORMATION
TECHNOLOGY
CTU IN PRAGUE

ASSIGNMENT OF BACHELOR'S THESIS

Title:	Application of Fourier and Wavelet Transform for Vibration and Acoustic Analysis of Machinery
Student:	Jan Lukány
Supervisor:	Ing. Tomáš Borovička
Study Programme:	Informatics
Study Branch:	Computer Science
Department:	Department of Theoretical Computer Science
Validity:	Until the end of summer semester 2018/19

Instructions

Machinery components (e.g. wind turbines or gearboxes) usually contain elements emitting vibration and acoustic signals. These signals often contain information that can reveal the condition of the component. Specific patterns, characteristic of different types of faults, are often easier to identify in the frequency domain. Therefore, spectral analysis methods are commonly used to analyse these signals. Fourier and Wavelet transforms are state-of-the-art methods for spectral analysis of signals in various domains.

1) Review and theoretically describe Fourier and Wavelet transforms and their usage in spectral analysis of time series.
2) Demonstrate the application of Fourier and Wavelet transforms on vibration and acoustic signals for condition monitoring of machinery components. Describe how the methods can reveal various defective conditions and verify it on real world data sets.

References

Will be provided by the supervisor.

doc. Ing. Jan Janoušek, Ph.D.
Head of Department

doc. RNDr. Ing. Marcel Jiřina, Ph.D.
Dean

Prague February 8, 2018

FACULTY
OF INFORMATION
TECHNOLOGY
CTU IN PRAGUE

Bachelor's thesis

Application of Fourier and Wavelet Transform for Vibration and Acoustic Analysis of Machinery

Jan Lukány

Department of Theoretical Computer Science
Supervisor: Ing. Tomáš Borovička

May 15, 2018

Acknowledgements

I would like to express my sincere gratitude to my supervisor Ing. Tomáš Borovička for his advices and mentorship. Also, I would like to thank my family and my friends for their endless support.

Declaration

I hereby declare that the presented thesis is my own work and that I have cited all sources of information in accordance with the Guideline for adhering to ethical principles when elaborating an academic final thesis.

I acknowledge that my thesis is subject to the rights and obligations stipulated by the Act No. 121/2000 Coll., the Copyright Act, as amended, in particular that the Czech Technical University in Prague has the right to conclude a license agreement on the utilization of this thesis as school work under the provisions of Article 60(1) of the Act.

In Prague on May 15, 2018 .....

Czech Technical University in Prague
Faculty of Information Technology

Citation of this thesis

Lukány, Jan. *Application of Fourier and Wavelet Transform for Vibration and Acoustic Analysis of Machinery.* Bachelor's thesis. Czech Technical University in Prague, Faculty of Information Technology, 2018.

Abstrakt

Většina mechanických zařízení vydává vibrační a akustické signály. Tyto signály mnohdy obsahují informace o oscilačním pohybu těchto zařízení, které mohou pomoci odhalit jejich aktuální stav, jakožto například že trpí závadou. Fourierova a Vlnková transformace jsou metody spektrální analýzy, jež dokážou reprezentovat signály pomocí oscilací a tedy jsou běžně používány pro zjišťování aktuálního stavu mechanických zařízení.

Tato práce popisuje Fourierovu a Vlnkovou transformaci a demonstruje jejich aplikaci ve vibrační a akustické analýze mechanických zařízení pomocí experimentů provedených na reálných datech. Výsledky experimentů potvrzují, že obě metody dokáží detekovat závadný stav mechanických zařízení. Přesněji, Furierova transformace může identifikovat přítomnost závady, kdežto Vlnková transformace dokáže i lokalizovat specifické vadné chování v čase.

Klíčová slova Fourierova transformace, Vlnková transformace, spektrální analýza, vibrační a akustická analýza mechanických zařízení

Abstract

Majority of industrial machinery emits vibration and acoustic signals. These signals often contain information about the oscillatory movement of the machinery that could reveal its condition, such as a defective state. Fourier and Wavelet transforms are spectral analysis methods which decompose signals into a representation by oscillatory functions. Thus, those methods are often used for condition monitoring of machinery.

This Thesis describes Fourier and Wavelet transforms and demonstrates their application for vibration and acoustic analysis of machinery on experiments conducted upon real-world data sets. The results of the experiments verify that both of the methods can distinguish different conditions of a machinery. Specifically, the experiments show that Fourier transform can identify a defective condition while Wavelet transform can even localize specific defective behavior in time.

Keywords Fourier transform, Wavelet transform, spectral analysis, vibration and acoustic analysis of machinery

Contents

List of Figures

Introduction

An industrial machinery often contains essential components which are under permanent stress. If they malfunction, the machine will stop or will not work correctly which could have a significant negative impact in production. Therefore, the condition of such parts is monitored and when a developing fault is detected, an appropriate action can be taken. Majority of machinery elements emit vibration and acoustic signals, which can contain characteristic patterns that could reveal the condition of the machine. Therefore, vibration and acoustic analysis is a standard condition monitoring technique of machinery.

One of the ways to analyze vibration and acoustic signals is application of spectral analysis methods that could decompose a signal into a representation by oscillatory functions, where each function is given a magnitude (weight) forming a spectrum of the signal. Specific spectral analysis methods differ in how they decompose the signal and in the choice of the oscillatory functions. The spectral analysis itself then consists of interpreting the weights of specific oscillatory function in the signal's spectrum.

Fourier and Wavelet transforms are state-of-the-art spectral analysis methods in various domains. Both the transforms have been successfully applied for analysis of vibration and acoustic signals of machinery in many works [3],[5],[6],[7],[8],[9]. However, authors usually provide only a breif definition of the methods as they suppose the reader is already familiar with them.

Goals

The first goal of this Thesis is to describe the two state-of-the-art spectral analysis methods – Fourier and Wavelet transform. The second goal is to describe how the spectra of the vibration and acoustic signals emitted from the machinery can reflect its condition and verify it on real world data sets.

The main contribution of this Thesis is that it provides both theoretical and practical background for application of the spectral analysis methods.

We introduce the spectral analysis methods from their basics and conclude experiments upon real world data sets based on the theory defined in the first part of the Thesis. Thus, this work can serve as an introduction for anyone who is interested in spectral analysis methods and their application in vibration and acoustic analysis of machinery.

Organization of the Thesis

The Chapter 1 establishes necessary basics of signals and spectral analysis. Chapters 2 and 3 theoretically describe Fourier and Wavelet transforms. The Chapter 4 provides description of several most common machinery components, their characteristic frequencies and describes how defective conditions of those components can affect vibration and acoustic signals they emit. The Chapter 5 demonstrates the application of spectral analysis methods on three experiments conducted upon real-world signals obtained from different types of machinery components. The Thesis is then concluded in Chapter 6.

Chapter 1

Preliminaries

In this Chapter we provide definitions of some essential terms and operations which occur in the rest of this thesis.

1.1 Time Series and Discrete Signals

Time series is generally defined as a chronological sequence of observations in time [10]. By $x[n] \in \mathbb{R}$ we will denote an observation at time n of a time series x, where $n \in \{0, 1, 2, ..., N-1\}$. To N we will refer as the length of the time series. The same definition can be applied to discrete signals, therefore we will not distinguish between a time series and a discrete signal. By a signal, we will refer to a discrete signal, unless said otherwise.

1.2 Cross-correlation

Cross-correlation is a measure of similarity between two signals. It is common to measure similarity between a longer and a shorter signal – i.e. looking for a pattern in the longer signal. Therefore, cross-correlation has a parameter commonly called shift or lag which shifts one of the signals in time. The cross-correlation between a signal x of length N and a signal y of length M at lag n, where $N \geq M$, is then defined as

$$(x \star y)[n] \equiv \sum_{m} x[m]y[m+n]. \tag{1.1}$$

1.3 Convolution

Convolution is a modification of one signal by another signal of the same or smaller length. Convolution of signal x of length N with a signal y of length

M, where $N \geq M$, is a discrete signal of length N defined as

$$(x * y)[n] \equiv \sum_m x[m]y[n-m]. \tag{1.2}$$

Convolution is a similar operation to cross-correlation. Specifically, $(x * y)[n] = (x \star y')[n]$, where signal y' is signal y reversed in time – $y'[n] = y[-n]$.

1.4 Spectral Analysis of Signals

Spectral analysis involves decomposition of the signal as a chronological sequence of observations in time into oscillations of different frequencies or scales [11]. The motivation is, that sometimes the oscillations can better characterize the information in the signal.

Methods for spectral analysis then assign magnitudes (weights) to the specific oscillations by calculating their cross-correlation with the signal or by convolution of the signal with the oscillation.

Chapter 2

Fourier transform

Fourier transform (FT) is a spectral analysis method which decomposes a function into a sum of sine waves of different frequencies. In this Chapter, we will focus on two types of Fourier transform which decompose discrete signals – Discrete Fourier transform and Short-time Fourier transform. We will aim to provide neccessary background of Fourier transform for its practical usage in discrete signal analysis. Therefore, we will not dive deep into its mathematical concepts. Those can be found e.g. in [12], [13] or [14].

The first Section (2.1) provides an introduction to sine waves. The second Section (2.2) describes Discrete Fourier transform (DFT) which decomposes a signal into sine waves of the same length as the signal, thus giving us the frequency spectrum of the signal. Since some signals change in time (e.g. an acoustic signal of a song played on piano changes with every new key pressed) a modified version of DFT, called Short-time Fourier transform, has been developed which decomposes a signal into sine waves localized in time forming a time-frequency spectrum of the signal. Short-time Fourier transform is described in Section 2.3.

Both the frequency and the time-frequency spectrums might suffer from an unwanted effect called spectral leakage. Applying special window functions during the transform is a common method to reduce this effect. Spectral leakage and the specific window functions are described in Section 2.4.

Computation of DFT of signal of length N was widely considered as a task of complexity $\mathcal{O}(N^2)$. However, in 1965 an algorithm called Fast Fourier transform (FFT) was introduced to general public[1] which is capable of computing DFT of length N in time complexity $O(N \log N)$ [16].

[1] Even though the roots of FFT can be tracked back to Gauss in 1805 [15].

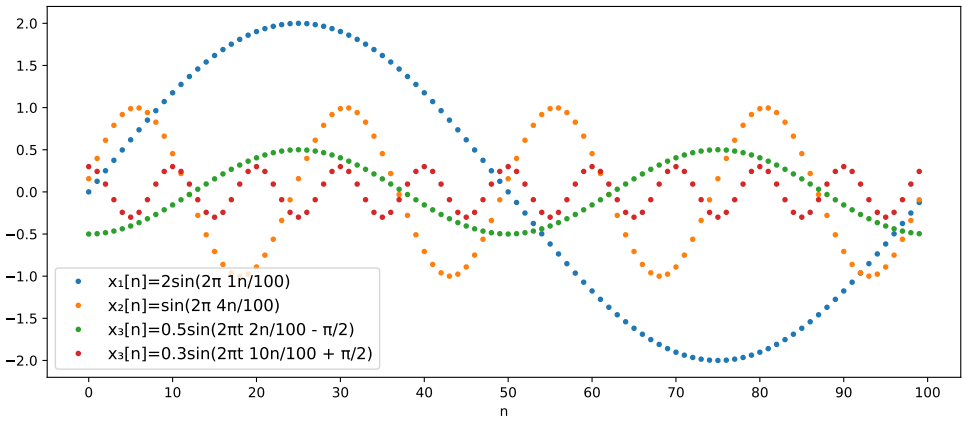

Figure 2.1: A few examples of discrete sine waves

2.1 Sine Waves

A sine wave is a function describing an oscillatory movement. A definition of a sine wave as a discrete signal x using a sine function is

$$x[n] = A\sin(\omega n + \varphi). \tag{2.1}$$

where the parameters are:

- ω – angular frequency: the duration of one oscillation in radians (when $\omega = 1$ the duration is 2π)
- A – amplitude: the height of oscillations
- φ – phase shift (or simply phase): the position where the start of oscillations is (at $t = 0$) with $\varphi \in (-\pi, \pi)$

The angular frequency of the sine wave can also be expressed as a number oscillations k per N time points in radians – $\omega = \frac{2\pi k}{N}$. We call k the ordinary frequency. With this notation, a sine wave can be defined as:

$$x[n] = A\sin\left[\frac{2\pi kn}{N} + \varphi\right]. \tag{2.2}$$

Figure 2.1 shows several discrete sine waves defined by the ordinary frequency.

Another way how to define a sine wave is by a linear combination of a sine and a cosine function of the same frequency [17]. The cosine function is a sine function shifted by a quarter of the oscillation ($\varphi = \frac{\pi}{2}$). The sine wave expresed by the sine and the cosine function is then defined as

$$x[n] = a\sin\left(\frac{2\pi kn}{N}\right) + b\cos\left(\frac{2\pi kn}{N}\right). \tag{2.3}$$

The amplitude a (b) can be seen as the amount of contribution of a sine (cosine) function to the sine wave. Specifically, the relations between a and b and the amplitude A and phase φ of the sine wave from definitions 2.1 and 2.2 are:

$$A = \sqrt{a^2 + b^2}, \tag{2.4}$$

$$tan(\varphi) = \frac{b}{a}. \tag{2.5}$$

The last definition of a sine wave is by the complex exponential. Using the Euler's formula

$$\mathrm{e}^{in} = \cos n + i \sin n \tag{2.6}$$

we are able to rewrite 2.3 as a complex discrete function $x : \mathbb{C} \to \mathbb{C}$

$$x[n] = c\mathrm{e}^{i\frac{2\pi kn}{N}}, \tag{2.7}$$

where c is a complex number with relation to the amplitude A and the phase φ of the sine waves from definitions 2.1 and 2.2 by equation:

$$A = \sqrt{\Re(c)^2 + \Im(c)^2}, \tag{2.8}$$

$$tan(\varphi) = \frac{\Im(c)}{\Re(c)}. \tag{2.9}$$

The definition of a sine wave by the complex exponential allows us to define a sine wave by only two parameters – the ordinary frequency k and complex amplitude c. Therefore, even if we work with real valued functions only, e.g. discrete signals, it is common to use this definition of a sine wave for convenience reasons.

2.2 Discrete Fourier transform

Any finite discrete signal x of length N can be expressed in a sum of sine waves by equation

$$x[n] = \sum_{k=0}^{N-1} c_k e^{i2\pi kn/N}, \tag{2.10}$$

where each complex coefficient c_k corresponds to a sine wave of frequency $\frac{2\pi k}{N}$. Discrete Fourier transform is then an operation that can tell us how to calculate the coefficients c_k given any signal x. The set of coefficients c_k for a function x is called the frequency spectrum of the function x.

In this Section, we will define DFT, show an example how a discrete signal can be decomposed into its frequency spectrum and we describe how to convert the ordinary frequencies k of the sine waves to the sampling rate of the discrete signal – i.e. express frequency k in Hz.

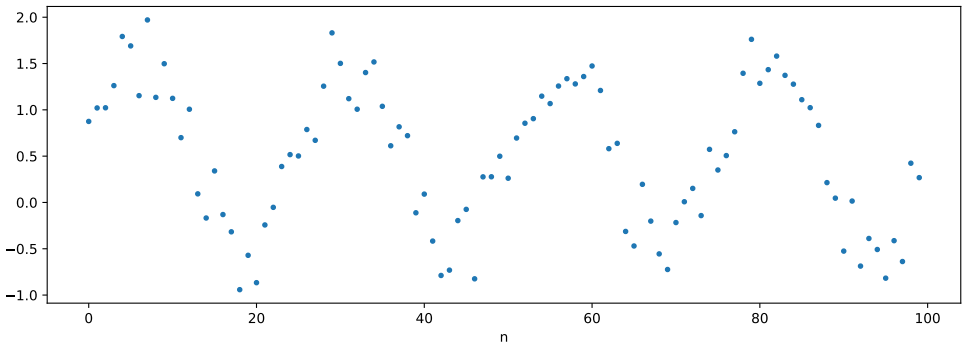

Figure 2.2: A discrete signal x of length $N = 100$.

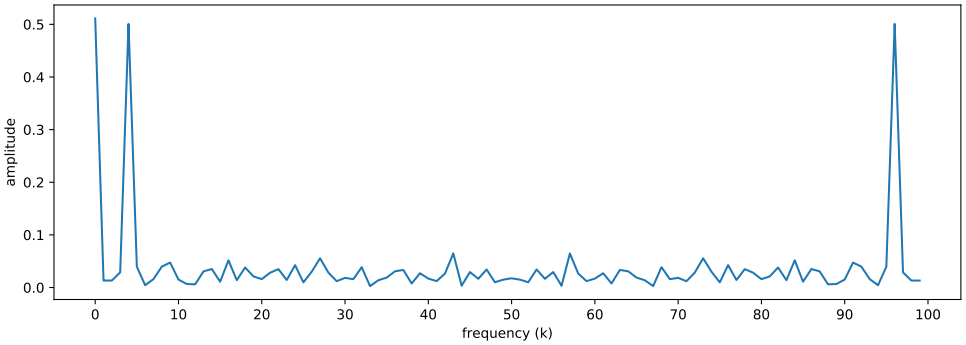

Figure 2.3: Amplitude and phase frequency spectras of signal x.

2.2.1 Definition

DFT is as linear transformation which transforms any finite discrete signal x of length N from a time domain into N complex coefficients $c_k, k \in \{0, 1, ..., N-1\}$ each representing a sine wave of frequency $\omega_k = \frac{2\pi k}{N}$. DFT of the signal x is defined as

$$c_k = \frac{1}{N} \sum_{n=0}^{N-1} x[n] e^{-i2\pi kn/N}. \tag{2.11}$$

2.2.2 Frequency spectrum

Figure 2.2 shows a discrete signal $x[n]$ of length $N = 100$. We see that the signal seems to follow a sine wave of frequency $\omega = \frac{2\pi 4}{100}$ oscillating around value 0.5. Figure 2.3 shows its amplitude frequency spectrum calculated from its coefficients c_k. We see a high peak at the frequency $k = 4$. Moreover, it contains peak of height around 0.5 at frequency k=0. A sine wave of frequency $\omega = 0$ is equal to one at all time points. Therefore, the amplitude of the frequency $k = 0$ in the signal's frequency spectrum is always equal to the

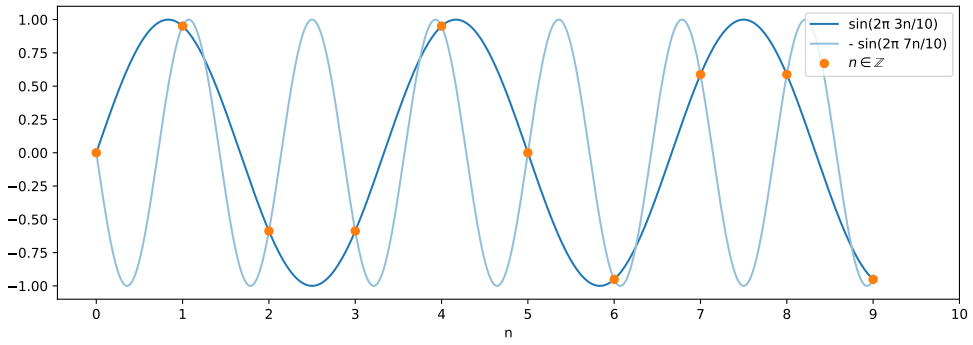

Figure 2.4: Continuous sine waves of different frequencies having the same values when discretized

average of the signal.

Notice that the frequency spectrum is horizontally symmetrical around the the frequency $N/2$. An important property of discrete sine waves is, that a sine wave of frequency $\frac{2\pi k}{N}$ has the same values as a sine wave of frequency $\frac{2\pi(N-k)}{N}$ except the sign. Figure 2.4 illustrates this property by showing two discrete sine waves and their continuous equivalent, where one is shown as negative. We see they have exactly the same values when discretely sampled. This leads to the fact, that in case of real-valued signals only $N/2$ sine waves are needed to fully represent it. Therefore, only frequencies up to $N/2$ are commonly shown in the frequency spectrum when working with real-valued signals.

Similarly, we can visualize phase spectrum which tells us how are the sine waves aligned. However, we are usually more interested in the amount of presence of the sine waves in the signal rather than their alignment.

2.2.3 Frequency normalization

Let us take an input signal x sampled at sampling rate $F_s = 50$Hz of length $N = 200$ (2 seconds) which has a periodic pattern recurring two times per second (2Hz). The amplitude spectrum of the signal x will have a high peak at frequency $k = 8$ oscillations per time interval $N = 200$ since the pattern is present 2 times per 50 samples. It is common to normalize the ordinary frequencies k with respect to the sampling rate of the signal. To do so we use the following formula:

$$f_k = \frac{F_s}{N} k. \tag{2.12}$$

The fraction $\frac{F_s}{N}$ tells us the spacing between the two consecutive frequencies k. The frequency f_k is then the frequency normalized with respect to the sampling rate F_s. In our case above, the length of the signal is 4 times the

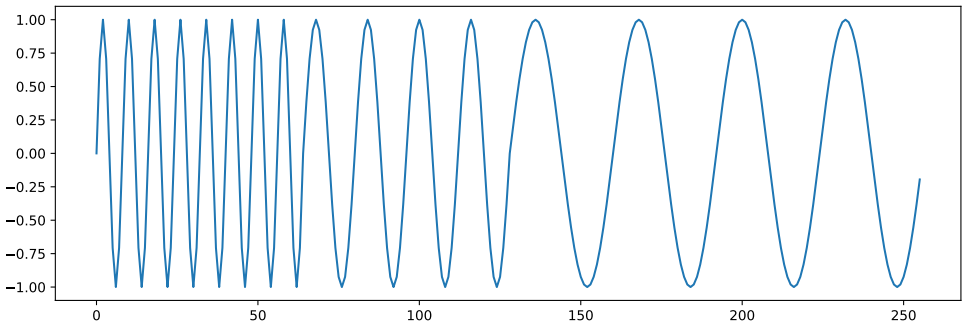

Figure 2.5: A signal changing its frequency spectrum during time.

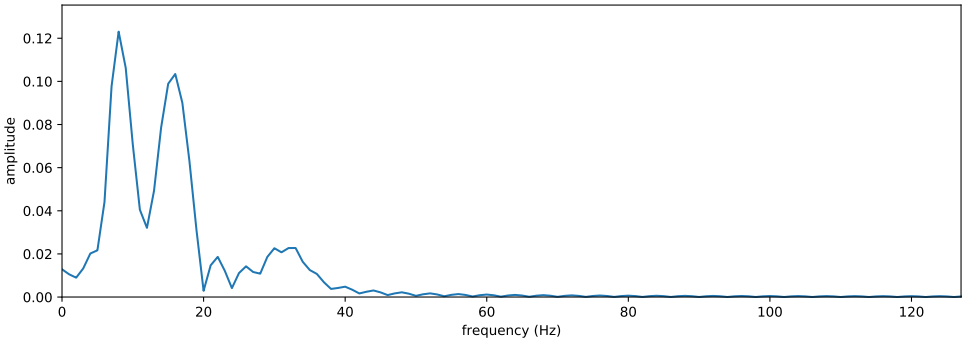

Figure 2.6: Frequency spectrum of the signal from figure 2.5.

sampling frequency – we have 4 seconds of the signal. Therefore each frequency k corresponds to $f_k = \frac{k}{4}$Hz.

2.3 Short-time Fourier transform

In the previous Section, we transformed a signal to its frequency domain assuming that its frequency spectrum does not change during time. However, frequency spectrum of some signals we encounter in real-world do change during time. Figure 2.5 shows a signal x of length $N = 256$ which contains a sine wave of frequency $f_1 = 2\pi\frac{32}{256}$ at the first quarter, frequency $f_2 = 2\pi\frac{16}{256}$ at the second quarter and $f_3 = 2\pi\frac{8}{256}$ at the last two quarters. Figure 2.6 then shows its frequency spectrum. We see the peaks at frequencies f_1, f_2 and f_3, but there is also a lot of contribution from other frequencies. This only roughly tells us which frequencies are present in the signal. However, we have no information about the localization of the frequencies in time which could be of high importance. Short-time Fourier transform is trying to solve this issue by using time localized sine waves.

Short-time Fourier transform decomposes a signal into M frequency spec-

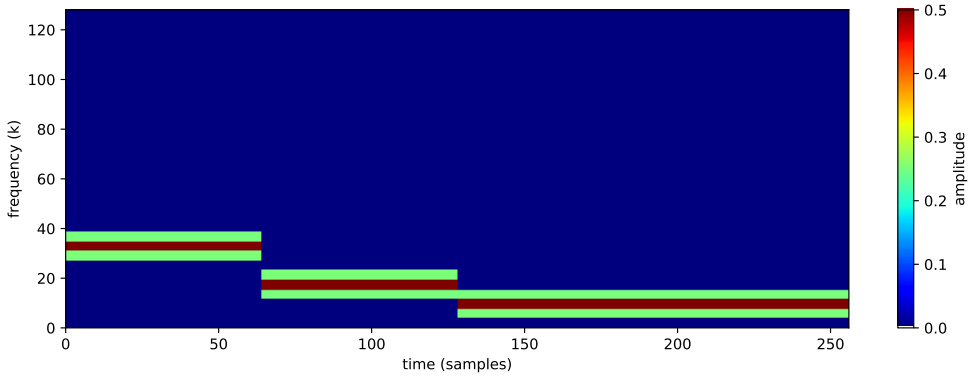

Figure 2.7: Spectrogram of the signal x from figure 2.5.

trums which together form the time-frequency spectrum of the signal. For each of the M frequency spectra, one chunk of the input signal is processed. The size of the chunk and the division of the signal into the chunks is done via a window function w which is nonzero for only a short period of time – it has a small support. The simplest window function if the square window, or the flat top window, defined as:

$$w[n] = \begin{cases} 1 & \text{if } n \in [0, l] \\ 0 & \text{otherwise} \end{cases} \tag{2.13}$$

where l is a parameter of the window function – the length of the non-zero interval (support).

STFT has two parameters k and m where k is the ordinary frequency of a sine wave and m is the translation of the window function in time. STFT of a function x is defined as:

$$\mathrm{STFT}_x[k, m] = \sum_{n=0}^{N-1} x[n]w[n-m]e^{-i2\pi kn/N}. \tag{2.14}$$

Figure 2.7 shows a spectrogram (time-frequency spectrum) for $m \in \{0, 64, 128, 192\}$ of the signal x from figure 2.5 with the square window function of length $t = 64$. We see that STFT localizes the signals's frequencies in time.

The size of the window function (the non-zero interval) is fixed for the whole computation. Therefore, choice of the window size is crucial in order to split the input signal to the chunks that correspond with the way the frequency spectrum changes during time.

Values of m can be chosen in a way that the translations of the window function overlap. Eg. in our case above choosing $m \in \{0, 32, 64, 96, ..., 224\}$ for the window w which is non-zero on interval $[0, 64]$ would lead to splitting the input signal into eight chunks where some values would be processed by STFT two times (eg. the interval $[32, 64]$). It is common to run STFT multiple

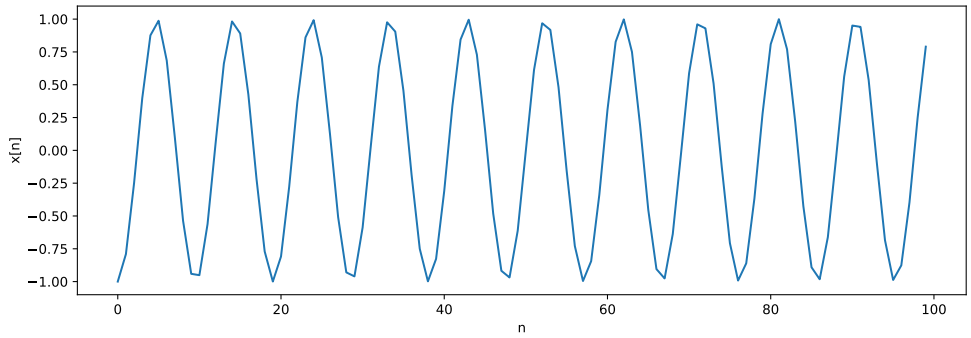

Figure 2.8: Signal of length $N = 100$ containing pattern sine wave of frequency $2\pi\frac{21}{200}$.

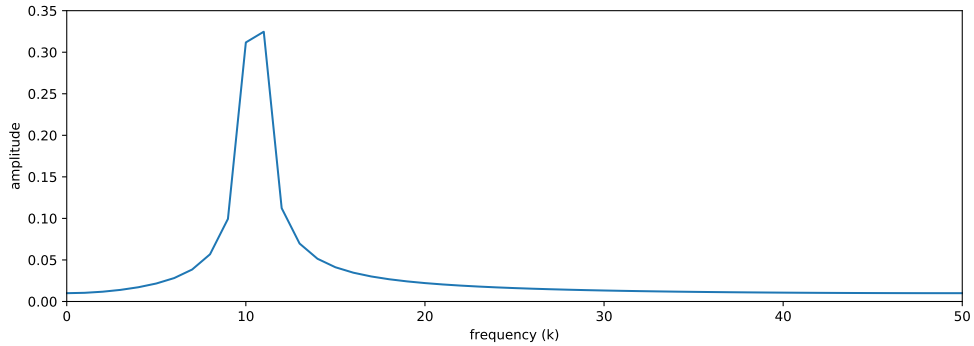

Figure 2.9: Frequency spectrum of the signal from figure 2.8.

times with different window sizes and different values of m and comparing the results in order to find the best parameters for the specific signal.

2.4 Spectral leakage

Both DFT and STFT use sine waves to describe the real-valued signal of length N. Each sine wave has frequency $\omega_k = \frac{2\pi k}{N}$ where $k \in [0, 1, ..., N/2]$ (in case of real valued input). However, it could happen that the signal contains frequency which is not equivalent to one of the listed frequencies. Figure 2.8 shows a signal x of length $N = 100$ consisting of a sine wave of frequency $f_0 = 2\pi\frac{21}{200} = 2\pi\frac{10{,}5}{100}$. DFT of this signal will contain frequencies $f \in \{2\pi\frac{0}{100}, 2\pi\frac{1}{100}, 2\pi\frac{2}{100}, ..., 2\pi\frac{10}{100}, 2\pi\frac{11}{100}, ..., 2\pi\frac{50}{100}\}$. Our frequency f_0 is right in between two frequencies of DFT. The frequency spectrum in figure 2.9 shows what happens – several sine waves near the frequency f_0 have high amplitude (the frequency f_0 leaks to the adjacent frequencies). This effect is called spectral leakage. It is an unwanted effect and because it biases the frequency spectrum it is desirable to reduce it.

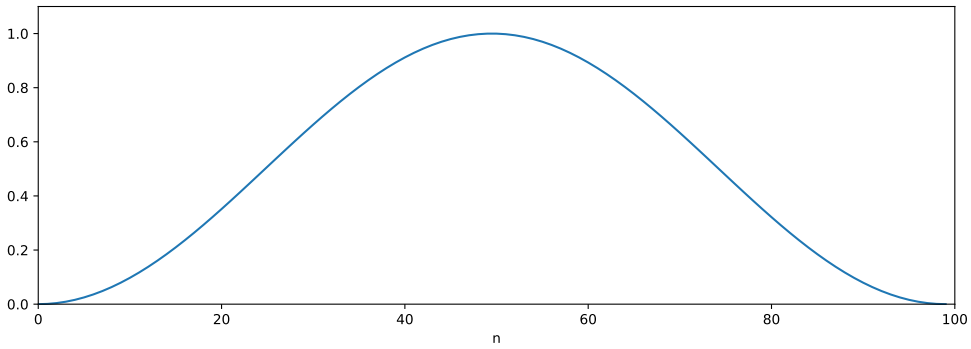

Figure 2.10: Hanning window function.

The most straight-forward way how to reduce the spectral leakage is by removing its source – the inability of DFT/STFT to cover all the frequencies. That could be done by taking a longer function we are analyzing which results in a higher density of the frequencies used by DFT and so higher chance that the frequencies used by DFT will be closer to the real ones in the signal. Eg. in the case shown above, extending the signal to length $N = 200$ makes the frequency f_0 to be contained in the frequency spectrum. However, sometimes we cannot or we do not want to take a longer signal – e.g. in STFT we want to analyze small chunks in order to have better time localization. In those cases, specific window functions can be used.

Window functions were already introduced in the previous section (2.3) where they were used to split the signal into the chunks (a square window function was used to perform that). The source of the spectral leakage can be also seen as the input signal not being periodic (it has unfinished oscillations). Therefore, specific window functions that reduce weight on the edges of the signal could reduce this negative effect. Figure 2.10 shows a Hann window function defined as:

$$w[n] = \frac{1}{2}\left(1 - \cos\left(\frac{2\pi n}{N-1}\right)\right), \tag{2.15}$$

where N is a length parameter.[2]

Figure 2.11 shows the frequency spectrum of the signal using no window function and using the Hanning window[3]. As seen, the spectral leakage is mostly reduced. The spectrum has high values only at two frequencies (at $f = \frac{10}{100}$ and $f = \frac{11}{100}$) which is accurate because the frequency present in the signal is right in the middle of them.

[2]We could apply a window function even in DFT – a DFT of length N can be seen as a special case of STFT where only one chunk with window length N is processed.

[3]Note that not applying any window function equals to applying a square window function. When we say no window function is used or we do not specify which window function is used, we will refer to using a square window function.

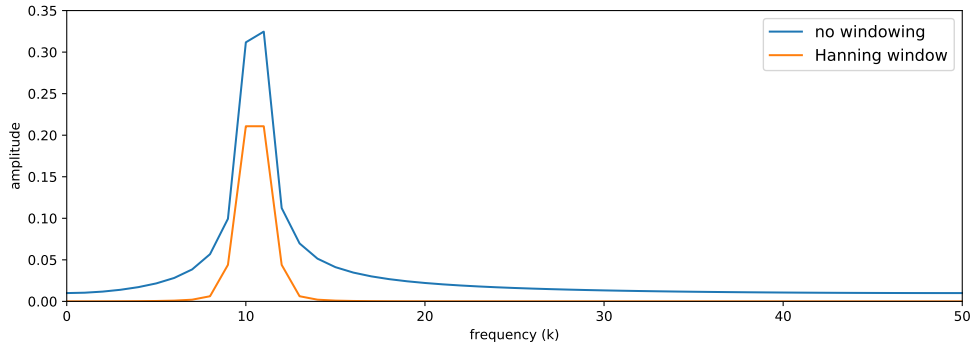

Figure 2.11: Frequency spectrum of the signal from figure 2.8 using Hanning window.

There are several established window functions including Hanning, Hamming, Kaiser-Bessel and Blackman-Harris [18]. They differ in a way how they assign weights to specific parts of the signal. Choice of the best performing window function is not a trivial task and is beyond the scope of this Thesis. We will use only Hanning window since it is sufficient in most applications.

Chapter 3

Wavelet transform

Wavelet transform (WT) is a spectral analysis method which decomposes a signal into a set of oscillatory functions called wavelets. The wavelets are localized in time and thus WT provides a time-frequency representation. It is an operation similar to Short-time Fourier transform but it is younger – engineers started using WT for signal analysis and processing in the late 20^{th} century. Therefore, in the first Section (3.1) we give a motivation example – analysis of a signal where STFT does not perform ideally and we describe how WT is supposed to solve this.

In this Chapter, we will focus on two types of Wavelet transform which are commonly used for signal analysis – Continuous Wavelet transform (CWT) and Discrete Wavelet transform (DWT). Despite its name, CWT is often used for discrete signal analysis. It provides a redundant representation of a signal in terms of scaled and translated wavelets derived from a continuous function called the mother wavelet. CWT is described in the second Section (3.2) of this Chapter. DWT, on the other hand, provides a non-redundant representation of a signal by a set of discrete orthonormal wavelets. DWT is described in the third Section (3.3) of this Chapter.

The focus of this Chapter is to provide neccessary background for practical application of CWT and DWT. Thus, we will not dive deep into mathematical concepts of Wavelet transform. Those are in detail described in many books written by experts in Wavelet domain [19], [20], [21], [22], [12]. Except those, we also recommend [23], [24], [25] and [26] as they can help understand Wavelet transform in more depth.

3.1 Introduction

In this section, we introduce the concept of Wavelet transform by a motivation example. The example consists of an analysis of a discrete signal by Short-time Fourier transform, which, however, will not give satisfying results and we explain how Wavelet transform is supposed to improve it. In the following

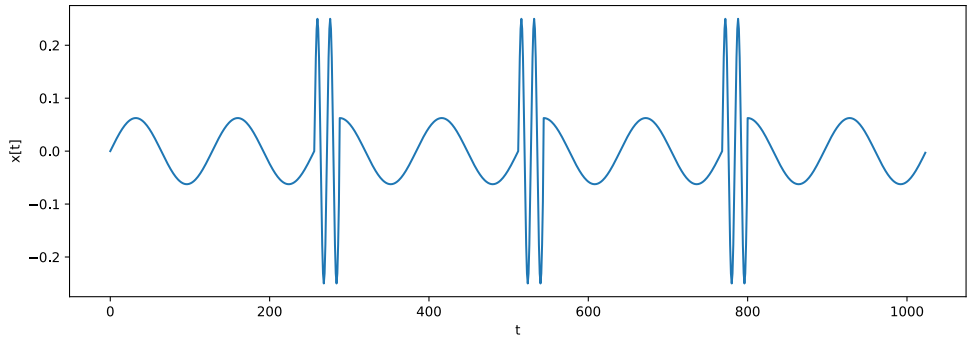

Figure 3.1: Signal x of length $N = 1024$

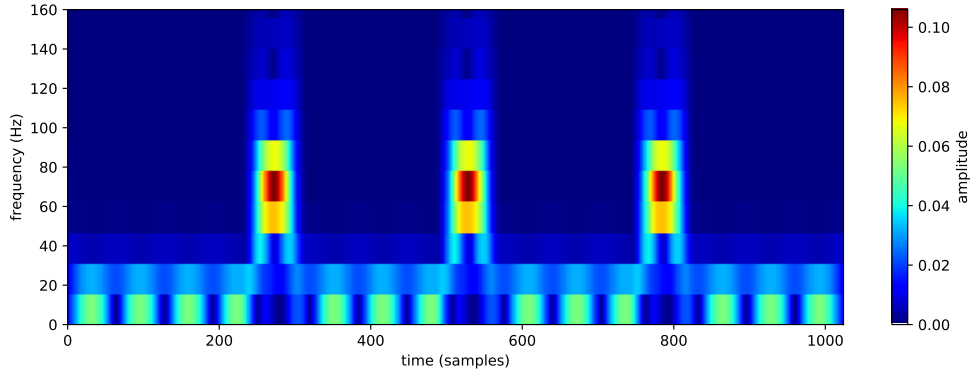

Figure 3.2: STFT with window length 64 and overlap 63 samples

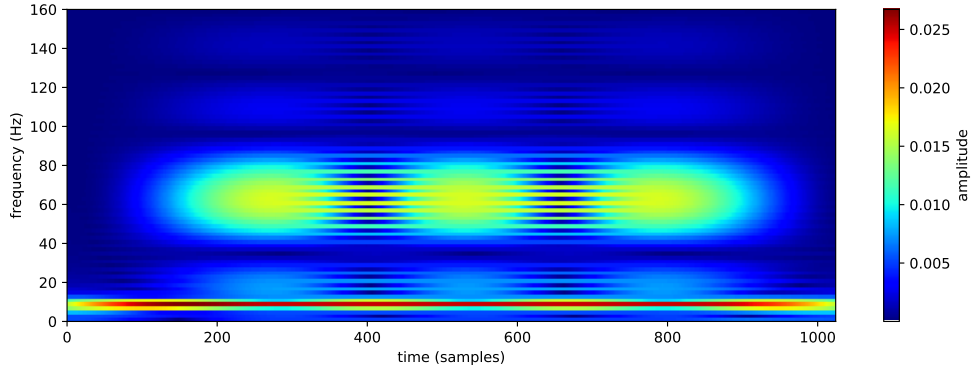

Figure 3.3: STFT with window length 512 and overlap 511 samples

section of this Chapter, the signal from this example will be analyzed by Continuous and Discrete Wavelet transform.

Figure 3.1 shows a discrete signal x of length $N = 1024$ with sampling rate $F_s = 1024$Hz. The signal consists of a sine wave of frequency 8Hz (low frequency pattern) and a sine wave of frequency 64Hz (a high frequency pattern). The low frequency pattern is present in the whole signal except for three short intervals where only the high frequency pattern is present. Short-time Fourier transform seems as an ideal choice since the signal has different frequency spectrum among different time intervals.

Figure 3.2 shows spectrogram of the signal using the square window of length 64 and overlap 63. From the spectrogram, we are able to localize the high frequency sinusoid in time. We can as well identify, that there is a low frequency pattern among the whole signal. However, we have relatively coarse resolution of frequencies – we can identify that the high frequency pattern is somewhere between 60 and 80Hz and the low frequency pattern somewhere between 0 and 20Hz. To achieve higher frequency resolution, we can increase the length of the window.

Figure 3.3 shows a spectrogram of the signal using the square window length 512 and overlap 511. In this spectrogram, we can clearly identify that the low frequency pattern is of frequency 8Hz. In case of the low frequency pattern, we now have a better estimate about its frequency as well – somewhere between 60 and 70Hz. However, we have now coarser time resolution.

To summarize, both spectrograms give us interesting information – the first localized the high frequency pattern in time and the second gave us good frequency localization of the low frequency pattern. In the real world, this is the usual kind of information we want – good time resolution at high frequencies and good frequency resolution at low frequencies. Wavelet transform does exactly this by an operation of scaling.

Wavelet transform represents a signal by a set of wavelets – oscillatory functions with compact support. The set of wavelets is derived from a function called the mother wavelet, commonly denoted as ψ, by scaling and translation. Figure 3.4a shows real part of the Morlet wavelet. The Morlet wavelet is defined as a complex exponential multiplied by a Gaussian function. Therefore, it can be seen as a special case of STFT when Gaussian function is chosen as the window function. Figure 3.4b shows what happens if we increase the frequency of the complex exponential in STFT. Figure 3.4c then shows what happens when we scale down the Morlet wavelet. This is the key difference between the concept of STFT and WT. Loosely speaking, WT using the Morlet wavelet is like STFT where we shrink the window size while increasing frequency. In Wavelet transform, this operation is called scaling. The scaling operation allows us to achieve good frequency resolution at low frequencies while having good time resolution at high frequencies.

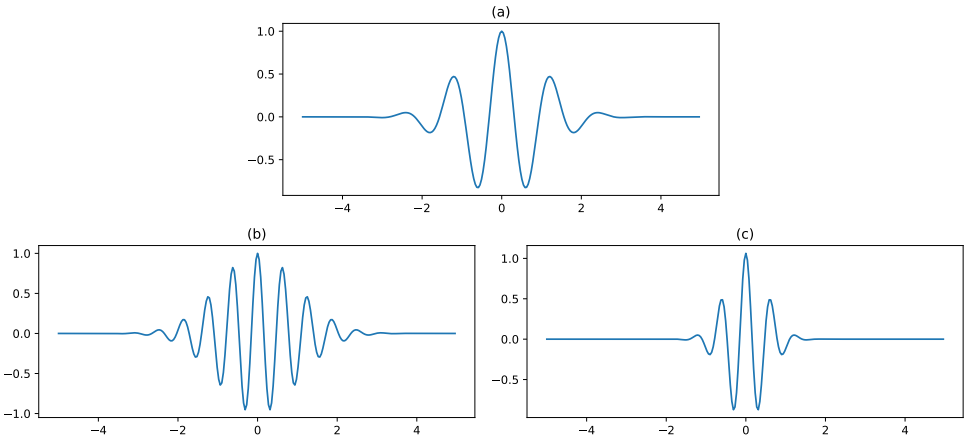

Figure 3.4: (a) real part of the Morlet wavelet, (b) higher frequency, (c) lower scale

3.2 Continuous Wavelet Transform

Continuous Wavelet transform provides a redundant representation of a function in terms of scaled and translated wavelets derived from the mother wavelet. A brief mathematical definition of CWT is provided in Subsection 3.2.1 along with a few examples functions that can be used as the mother wavelet. In order to be implemented on a computer, CWT has to be discretized. Therefore, the discretization of CWT is described in Subsection 3.2.2. The third Subsection (3.2.3) analyzes the signal from the previous Section by CWT. The last Subsection (3.2.4) briefly describes computational complexity of CWT.

3.2.1 Definition

CWT represents a signal by scaled and translated wavelets $\psi_{s,\tau}$ derived from the mother wavelet ψ by equation

$$\psi_{s,\tau}(t) = \frac{1}{\sqrt{s}}\psi\left(\frac{t-\tau}{s}\right). \tag{3.1}$$

Figure 3.5 shows a few scaled and translated versions of the Morlet wavelet. The parameters s and τ are called scale and translation. CWT of a continuous and well behaved[4] function f is defined as

$$\mathrm{CWT}_\psi(s,\tau) = \int_{-\infty}^{\infty} f(t)\psi^*_{s,\tau}(t)dt, \tag{3.2}$$

where $s \in \mathbb{R}^+$, $\tau \in \mathbb{R}$, ψ is the mother wavelet and ψ^* is the complex conjugate of ψ.

[4]The function has to be from $\mathcal{L}^2$ space.

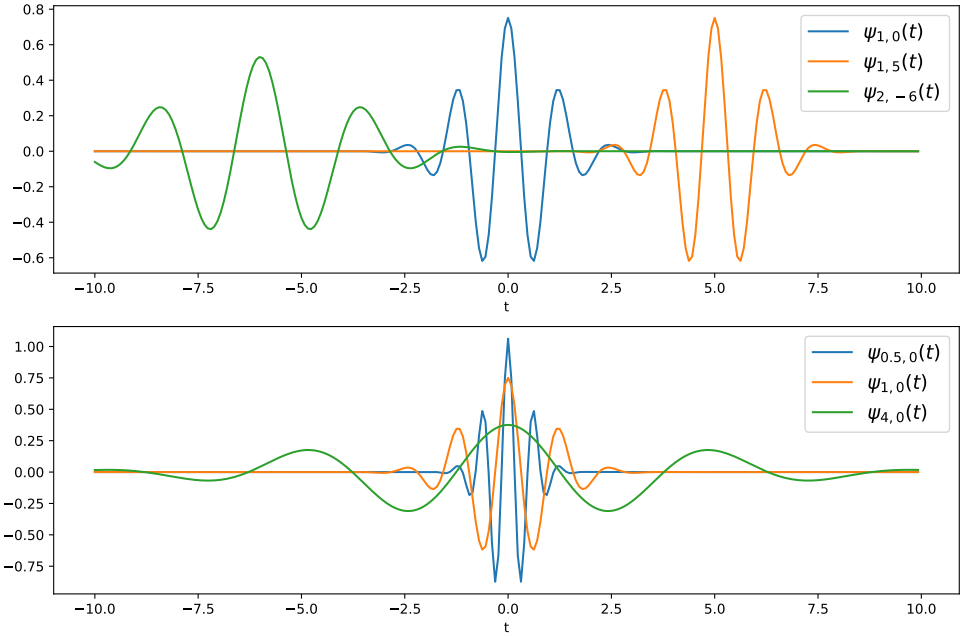

Figure 3.5: Scaled and translated wavelets derived from Morlet wavelet

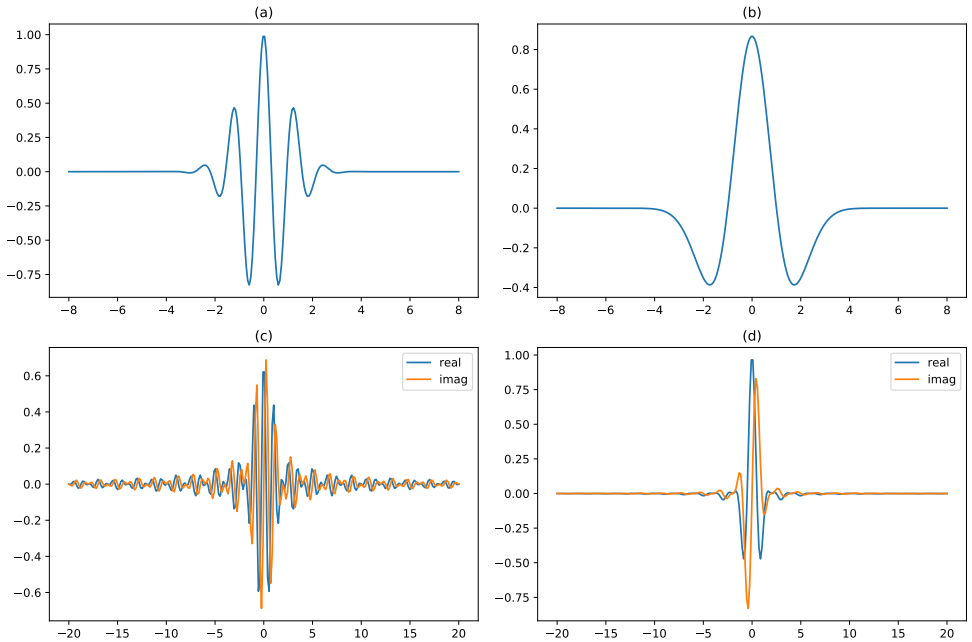

Figure 3.6: Examples of admissible wavelets: (a) real-valued Morlet wavelet, (b) Mexican hat wavelet, (c) Shannon wavelet, (d) fbsp wavelet (B-spline)

In order for the transform to be inversible, the mother wavelet has to satisfy the admissibility condition [20]. Definition of the admissibility condition and the inverse formula for CWT is, however, beyond the scope of this thesis. For our purpose, it is enough to say that the admissibility condition implies that the mother wavelet has to be compactly supported and has to be oscillatory around zero – hence the term wavelet. Application of CWT usually does not involve reconstruction of the signal from its coefficients. However, the inversibility of the operation guarantees us that all the information from the original signal, is also present in its CWT. Therefore, even though the reconstruction is not necessary, admissible wavelets are commonly used. Figure 3.6 shows a few admissible wavelets.

As seen in the Figure 3.6, different mother wavelets can have different width (support). Therefore, the scale parameter depends on the mother wavelet and it can be difficult to interpret it. As illustrated at the beggining of this Chapter, scale is closely related to frequency. Thus, it is common to approximate frequencies of the scaled wavelets. The approximation is possible using the central frequency of the scaled wavelet [27]. E.g. the central frequency of the Morlet wavelet is defined as the position of the global maximum of its Fourier transform [28].

3.2.2 Discretization

By definition, CWT is calculated for infinite number of scales and translations. In this section, we will describe how to discretize both scales and translations of CWT in order to be applicable on finite discrete signals.

CWT of a finite discrete signal consists of N translations and M scales. The amount of translations N is usually set to be equal to the length of the signal and the translation values are chosen to correspond with the sampling rate of the signal. E.g. if we have a signal of length N, we choose translations $\tau \in \{0, 1, ..., N-1\}$. The discretization of scales into M values then consists of two steps – selection of the range of scales and discretization of that range.

The range of scales can be set to cover all frequencies present in the signal based on the convertion between the scale and frequency. However, with the amount of scales raises the computational complexity. Therefore, there are several methods how to discretize a selected range of scales.

The selected range of scales can be discretized by linear sampling – e.g. from the range $s \in [1, 16]$ we take $\{1, 2, 3, 4, ..., 16\}$. However, the scaling equation (3.1) results in the fact that the difference in size between two low scale wavelets is much higher than the difference between two high scale wavelets. In other words, the scaling of the wavelets is logarithmic. Therefore, it is common to discretize the scale range exponentially [29]. The scales are discretized dyadically. the scaling equation for the wavelets then becomes

$$\psi_{j,\tau}(t) = \frac{1}{\sqrt{2^j}} \psi \left(\frac{t - \tau}{2^j} \right).$$

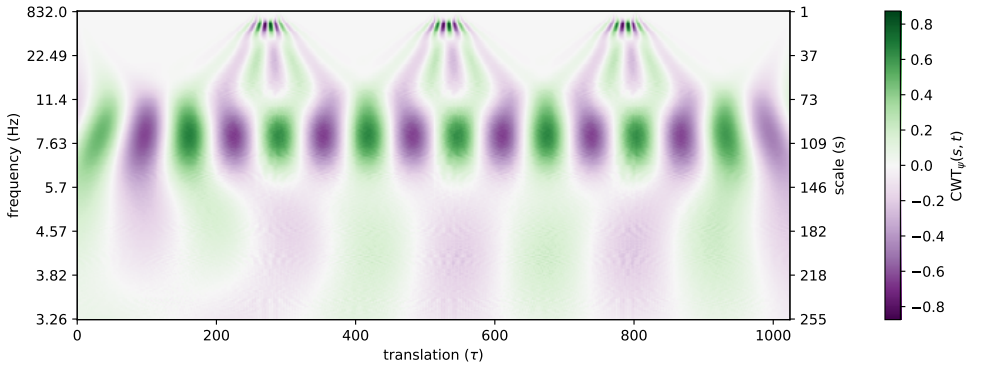

Figure 3.7: Scalogram of the signal from Figure 3.1 with linear sampling of the scale range

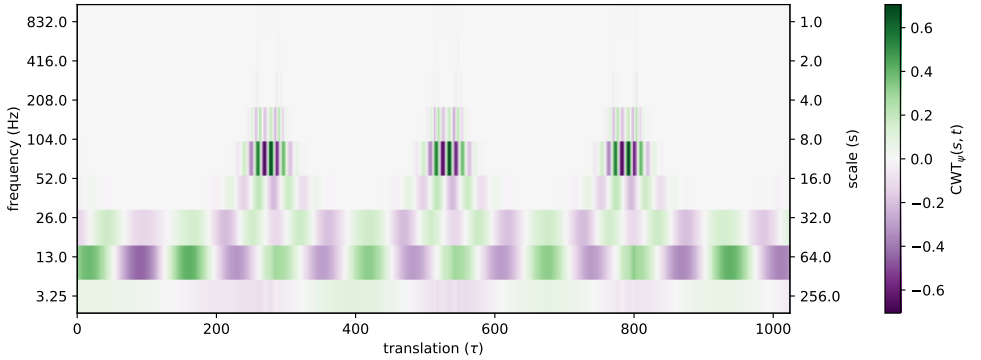

Figure 3.8: Scalogram of the signal from Figure 3.1 with dyadic sampling of the scale range

The dyadic scaling results in a very coarse discretization of scales. Therefore, it is common to pick the base as some root of two – $2^{1/v}$. The scaling equation then becomes

$$\psi_{j,\tau}(t) = \frac{1}{\sqrt{2^{j/v}}}\psi\left(\frac{t-\tau}{2^{j/v}}\right).$$

When we take twice the higher parameter v, the resolution becomes twice finer. The parameter v is often reffered to as the number of voices per octave [30].

3.2.3 Signal Analysis

A common way how to visualize the coefficients of CWT is by a scalogram. The scalogram is a three dimensional visualization which usually shows scale on the vertical axis, translation on the horizontal axis and $\mathrm{CWT}_\psi(s,\tau)$ as a

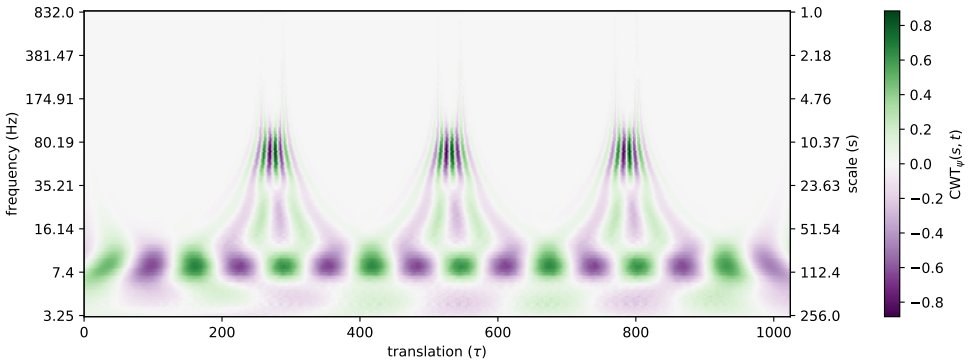

Figure 3.9: Scalogram of the signal from Figure 3.1 with exponential sampling of the scale range with base $2^{1/16}$

color from a color range[5]. The scale is often converted to frequency. Then, either only the frequency is displayed on a vertical axis or the scalogram has two vertical axes.

Figures 3.7-3.9 shows scalograms of the signal from the motivation example at the beginning of this Chapter for scale range $s \in [1, 256]$ using a real valued Morlet wavelet. Each of the figures shows different discretization of the scale range, namely linear, dyadic and with base $2^{1/16}$.

When we fix the scale parameter s, the equation 3.2 can be interpreted as a cross-correlation between the signal and translated wavelet ψ of scale s at lag τ [22]. The value of $\mathrm{CWT}_\psi(s, \tau)$ can be then interpreted as the amount of similarity between the signal and the wavelet $\psi_{s,\tau}$ or in other words – amount of presence of the pattern similar to the wavelet $\psi_{s,\tau}$ in the signal. Therefore, in the scalogram, we are usually interested in both coefficients with high negative values and high positive values.

3.2.4 Computation Complexity

Calculation of CWT coefficients for one scale can be realized by a convolution operation. Since convolution of two signals can be computed by the FFT algorithm with complexity $O(N \log N)$, the calculation of CWT for M scales and N translations yield complexity of $O(MN \log N)$.

3.3 Discrete Wavelet Transform

Discrete Wavelet transform (DWT) is an operation of decomposing a signal into a set of discrete orthonormal wavelets. It was first introduced by hungarian mathematician Alfred Haar [31], however, back then he did not call

[5]When a complex function is used as the mother wavelet, the coefficients of CWT becomes complex numbers. In that case, it is common to show amplitude and phase scalograms.

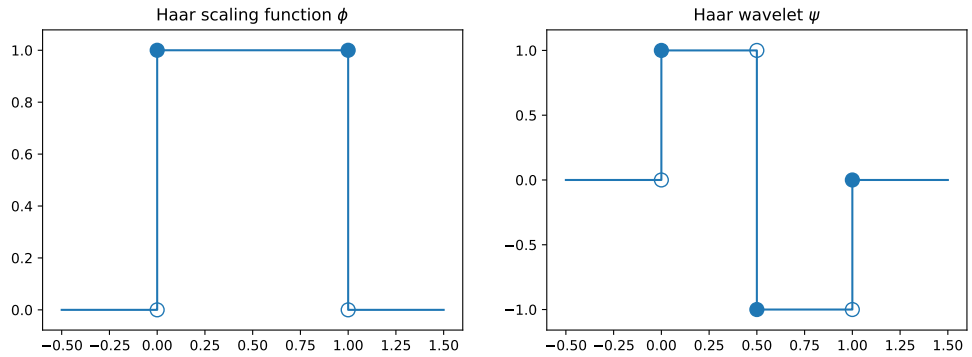

Figure 3.10: Haar scaling function and Haar wavelet

it Discrete Wavelet transform yet. The advent of DWT came with Ingrid Daubechies's introduction of a family of orthonormal wavelets [32]. Moreover, Stephen Mallat introduced an algorithm called Fast Wavelet transform capable of computing DWT with complexity $O(n)$ [33]. We give an introduction to general concept of DWT in the first Subsection (3.3.1) in a form of comparison with CWT. In the second Subsection (3.3.2) we briefly describe how the decomposition of a discrete signal is realized by DWT. The last Subsection (3.3.3) describes how can be the mentioned computation complexity $O(N)$ achieved.

3.3.1 Concept

CWT was discretized by exponential sampling of scales while the amount of translations was fixed – equal to the length of the analyzed signal. However, we can have coarser time resolution at higher scales than on lower scales while capturing the same amount of information. In other words, we can reduce the amount of translations at higher scales. DWT does exactly this by dyadic sampling of both scale and translation. The dyadic sampling of translations is then commonly called dilation. In DWT, the wavelets $\psi_{j,k}$ derived from the mother wavelet ψ are scaled and dilated by equation

$$\psi_{j,k}(t) = \frac{1}{\sqrt{2^j}}\psi\left(\frac{t - 2^j k}{2^j}\right) = 2^{-j/2}\psi(2^{-j}t - k). \tag{3.3}$$

Another difference of DWT from CWT is, that the wavelets used in DWT are discrete. Moreover, the mother wavelet ψ is defined by a scaling function ϕ, commonly called the father wavelet, by equation

$$\psi[n] = \sum_k (-1)^k g[k]\phi[2n - k]. \tag{3.4}$$

The scaling function ϕ has to satisfy the following recursive condition:

$$\phi[n] = \sum_k h[k]\phi[2n-k]. \tag{3.5}$$

The discrete signals h and g are called the high pass and low pass analysis filters of the scaling function ϕ and the mother wavelet ψ. Figure 3.10 shows Haar scaling function and Haar mother wavelet.

3.3.2 Fast Wavelet transform

Fast Wavelet transform decomposes a finite discrete signal x of length N into detail and approximation coefficients in form of discrete signals and total length of N. It consists of successive decomposition steps called levels using the high pass and the low pass analysis filters of the scaling function ϕ and the mother wavelet ψ. The first level of decomposition of a signal x containing frequencies $[0, f]$ is defined as

$$\begin{aligned} \mathrm{cD}_1[n] &= (x * h)[n] \downarrow 2, \\ \mathrm{cA}_1[n] &= (x * g)[n] \downarrow 2, \end{aligned}$$

where $\downarrow 2$ denotes subsampling by two (discarding every second value) and h and g are the high pass and the low pass analysis filters. $\mathrm{cD}_1[n]$ contains frequencies $[f/2, f]$ of the signal x and is commonly called level 1 detail coefficient. $\mathrm{cA}_1[n]$ contains frequencies $[0, f/2]$ of the signal x and is commonly called level 1 approximation coefficient. The level k approximation coefficient cA_k can be further decomposed into level $k+1$ detail and approximation coefficients by another convolution with the high pass and the low pass filters and downsampling:

$$\begin{aligned} \mathrm{cD}_{k+1}[n] &= (\mathrm{cA}_k * h)[n] \downarrow 2, \\ \mathrm{cA}_{k+1}[n] &= (\mathrm{cA}_k * g)[n] \downarrow 2. \end{aligned}$$

The original signal x can be then reconstructed back from its coefficients cD_1, cD_2,..., cD_k and the coefficient cA_k.

Figure 3.11 shows six levels of decomposition of a signal x from Figure 3.1 from the beggining of this Chapter. The detail coefficients are often visualized in scalogram. The scalogram of the whole decomposition of the signal (up to level 10) is shown in Figure 3.12.

3.3.3 Computation Complexity

Each level of decomposition consists of two convolution operations. Convolution operation has by definition a complexity of $O(N * M)$ where N and M are lengths of the signals being convolved. If the filters h and g are finite, which e.g. in case of Haar wavelet are, then the complexity of the first level

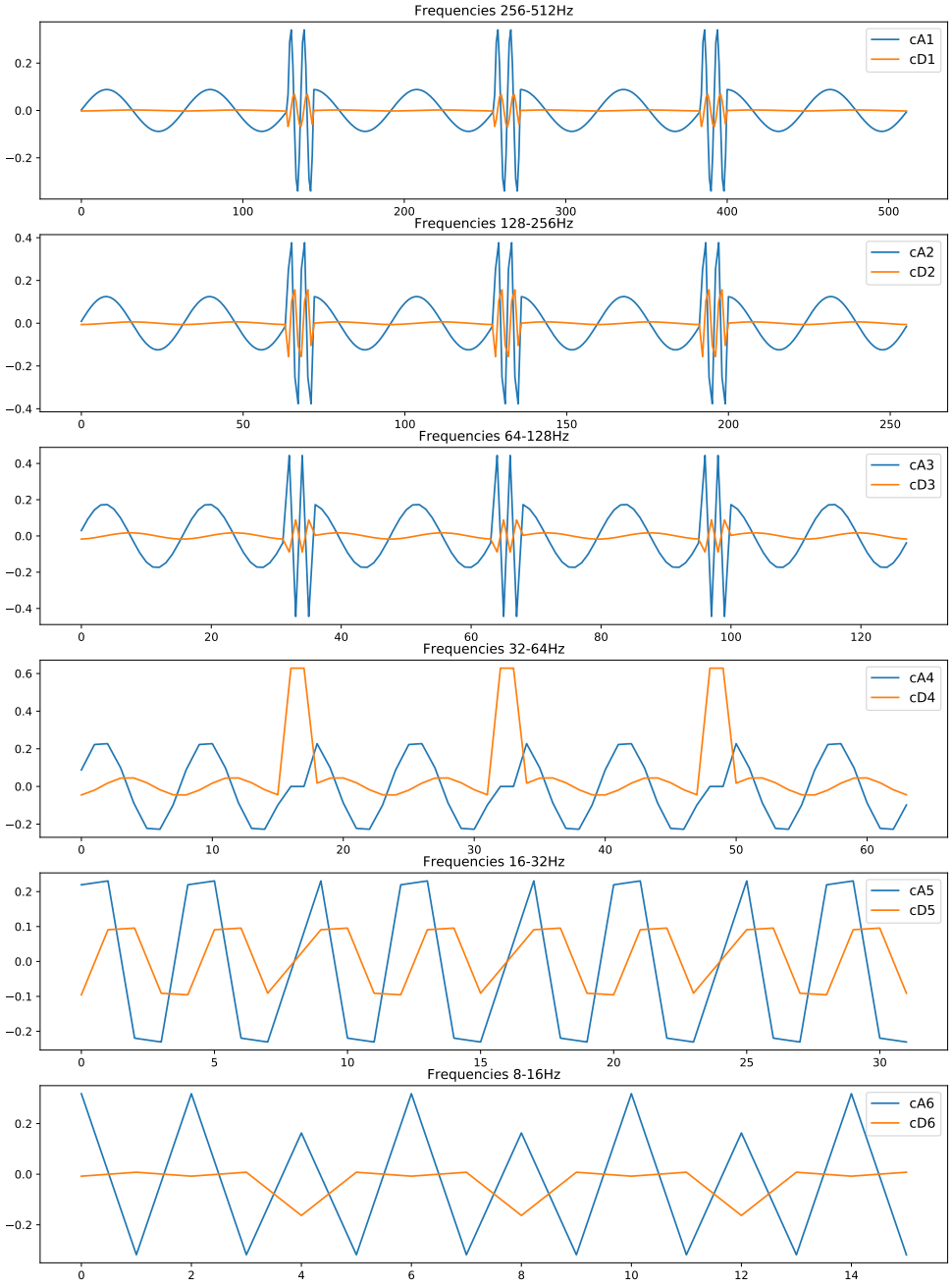

Figure 3.11: DWT decomposition of the signal from Figure 3.1 on detail and approximation coefficients using Haar wavelet

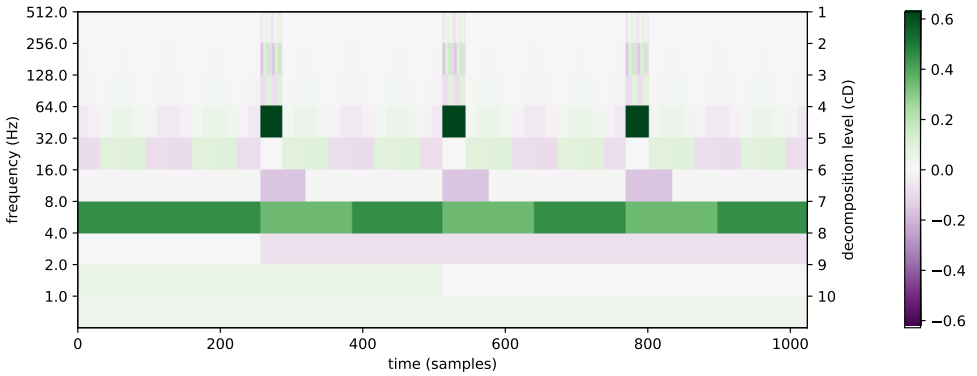

Figure 3.12: DWT using Haar wavelet of the signal from Figure 3.1

of decomposition is $O(2N)$ where N is the length of the input signal of DWT. The k-th level of decomposition is then of complexity $O(N/2^{k-1})$. This leads to a reccurence relation $T(N) = 2N + T(N/2)$ which yields $O(N)$.

Chapter 4

Vibrations and acoustic emissions of machinery

This chapter established necessary background of vibration and acoustic signals the machinery emit and its characteristics. The first Section (4.1) describes the signals and how they can be acquired from the machinery. The second Section 4.2 describes basic machinery elements and characteristics of their vibrations and acoustic emissions. The third Section (4.3) describes how the signals of a healthy and a faulty machine could differ and how that knowledge can be used to determine the condition of a machine.

4.1 Data acquisition

Both vibration and acoustic emission contain information about oscilatory movement of molecules in space (mechanical waves) around a reference position. Vibration refers to the movement in a solid matter while acoustic emission refers to the movement in liquids and gases. The two signals are closely correlated since an oscillatory movement of a solid matter also generates acoustic waves and vice versa.

The data are acquired from sencors in a form of finite discrete signals. In case of acoustic emissions the sensor is a microphone placed near the machine and measuring the sound pressure level. In case of vibrations three types of sensors can be used: accelerometer, velocimeter and proximity probe measuring acceleration, velocity and displacement, respectively. Those sensors have to be physically connected to the machine.

4.1.1 Displacement, velocity and acceleration

Vibration data can be represented in three units – displacement, velocity and acceleration. Figure 4.1 shows frequency spectra of the same vibration signal in different units. Notice that in the frequency spectrum of displacement

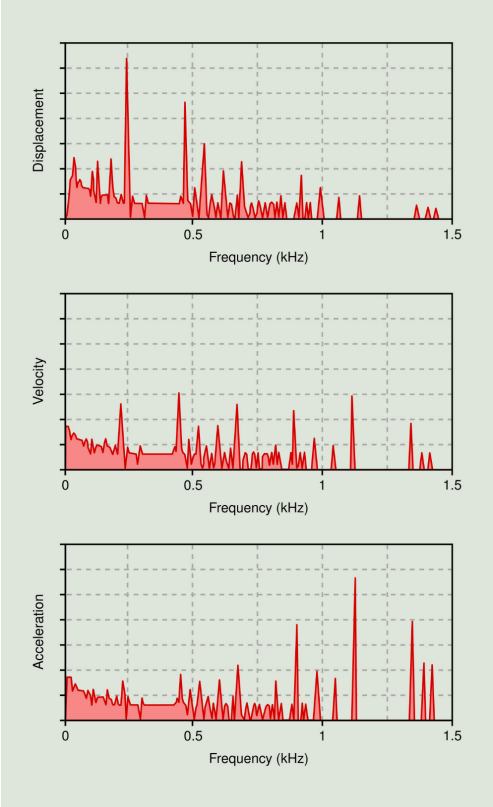

Figure 4.1: Frequency spectrum of different units of vibration data. Source: [1]

higher the frequency lower the amplitude and vice versa in the acceleration frequency spectrum. Level of amplitude in velocity frequency spectrum remains relatively same across the whole frequency spectrum. This is a common behaviour of most machinery parts.

Proximity probes are then commonly used for low frequency analysis. Since velocity provides detail in both low and high frequencies, it is the most convenient unit for general vibration analysis. However, usage of velocimeters is uncommon due to difficulties in their construction. The most common sensor for measuring vibrations is then an accelerometer, which can measure vibrations at high sampling rates and its construction is relatively easy.

4.2 Basic machinery elements and their characteristic frequencies

A machine is an apparatus which consumes power in order to apply forces and control movement. It usually consists of many parts (elements) such as

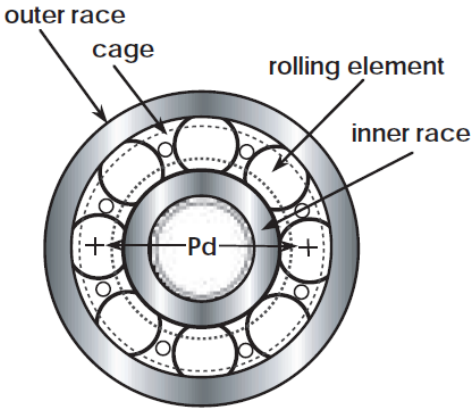

Figure 4.2: A ball bearing. Source: [2]

gears, bearings, valves and others. Each moving element emits vibrations and acoustic noise which contain characteristic frequencies based on the physical properties of the element and its speed of movement.

Majority of vibrations and acoustic noise in machinery is generated by rotating elements. Building a perfectly balanced rotating machine is hard to achieve. Therefore it often emits vibrations and acoustic noise at various frequencies called the characteristic frequencies. The first characteristic frequency of every rotating element of machinery is then the frequency equivalent to the speed of its rotation – the driving frequency. In most cases it is the speed of a shaft connected to the rotating element. We will denote it as F. Other characteristic frequencies are based on specific machinery element types and its properties. In this Section, we will describe three basic rotating machinery elements, which are the most common subjects of vibration and acoustic analysis – a bearing, a gear and a turbine.

4.2.1 Bearing

A bearing is a machinery element which reduces friction between two parts of the machinery. The most common type is a rolling element bearing, shown in Figure 4.2. The bearing is attached to two parts of the machinery via an outer and an inner race. The driving frequency of the bearing is the speed of movement between the outer and the inner race. A space between the races is filled with a cage containing rolling elements – most commonly balls — which allow an independent movement the races, and thus the machinery parts connected to it, at little friction.

Basic parameters of a ball bearing are [2]:

- Bn – number of balls
- Bd – ball diameter

- Pd – pitch diameter (distance between centers of the two opposite balls as shown in Figure 4.2)
- Θ – contact angle between a ball and the outer race

The characteristic frequencies of a ball bearing are then:

- CPF (cage pass frequency) = $\frac{1}{2}F\left[1 - \frac{\mathrm{Bd}}{\mathrm{Pd}}\cos\Theta\right]$
  - Frequency at which the cage with rolling elements fully spins itself.
- BSF (ball spin frequency) = $\frac{\mathrm{Pd}}{2\mathrm{Bd}}F\left[1 - \left(\frac{\mathrm{Bd}}{\mathrm{Pd}}\cos\Theta\right)^2\right]$
  - Frequency at which one ball fully spins itself.
- BPFO (ball pass frequency of the outer race) = $\frac{\mathrm{Bn}}{2}F\left(1 - \frac{\mathrm{Bd}}{\mathrm{Pd}}\cos\Theta\right)$
  - The lowest frequency at which two balls pass the same location at the outer race.
- BPFI (ball pass frequency of the inner race) = $\frac{\mathrm{Bn}}{2}F\left(1 + \frac{\mathrm{Bd}}{\mathrm{Pd}}\cos\Theta\right)$
  - The lowest frequency at which two balls pass the same location at the inner race.

4.2.2 Gear

A gear is a part of a machinery which transmits torque. It has cut teeth which mesh with another toothed part of a machinery and causes it to move. Multiple gears can be connected to each other making together a gearbox which provides torque conversion (transmission). When speaking of two gears connected to each other the smaller gear is usually refered to as a pinion.

A basic property of a gear is its number of teeth – n. A basic characteristic frequency of a gear is then the gear mesh frequency (GMF) defined as the number of teeth multiplied the driving frequency – $GMF = F * n$.

4.2.3 Turbine

A turbine is a rotating machinery which extracts energy from a fluid such as wind or water. It consists of a shaft connected with an assembly of blades. The fluid or the gas applies force to the blades which causes the turbine to move. The shaft of a turbine is then usually connected to a generator, which transforms that mechanical energy into electricity.

A basic property of a turbine is number of blades in its assembly – n. A basic characteristic frequency of a turbine is then the blade pass frequency (BPF) calculated as the number of blades multiplied by the driving frequency. BPF tells us the lowest frequency at which two blades pass the same position.

4.3 Condition monitoring

The set of frequencies contained in the vibration or acoustic signals emitted by the machinery usually consists of the machine's characteristic frequencies and other naturally occuring frequencies either of the machine itself or of its near environment. We call this set of frequencies emitted by the machinery at time t the spectral signature of the machine at time t. The time t can be a one time point or an interval between two time points depending on the context.

A machine can suffer from a wear after some time under operation which can be seen as a continuous degrading process. Moreover, a machine can suffer from a defect which might be as well continuously developing during some time due to eg. a fault in construction or onproper maintenance or it might be caused by a sudden accident such a shaft crack. Therefore, the spectral signature of the machine may vary in time. The main goal of condition monitoring is to detect these changes and decide whether the device is in a defective condition and how severe that condition is. This Section describes basic defects and wear conditions of rotating machinery elements described in the previous Section.

4.3.1 Unbalance, misalignment and looseness

Unbalance, misalignment and looseness are common defective conditions of a general rotating machinery. They are commonly related to the driving frequency of the rotating element causing the spectral signature to contain higher presence of the driving frequency (F), its harmonics (2F, 3F,...) or even its subharmonics (F/2,F/3,...) [6].

Unbalance is characterized by high presence of the driving frequency. Misalignment typically causes the rotating element to move in a shorter periodic pattern, thus it is often identified by higher presence of the driving frequency's harmonics, especially 2F [34]. Looseness might on the other hand cause the rotating element to move in longer periodic patterns and thus might be connected with subharmonics of the driving frequency. Figure 4.3 shows example frequency spectrums of a healthy rotating machine (unfault) and a machine suffering from unbalance, misalignment and looseness.

Sometimes identifying exact type of the fault can be difficult, especially between misalignment and looseness. The vibration and acoustic data can be then measured at several places on the machinery and in different directions, e.g. radial and axial. Analysis of the differences between the spectral signatures obtained from different places or directions may then distinguish the faults [1].

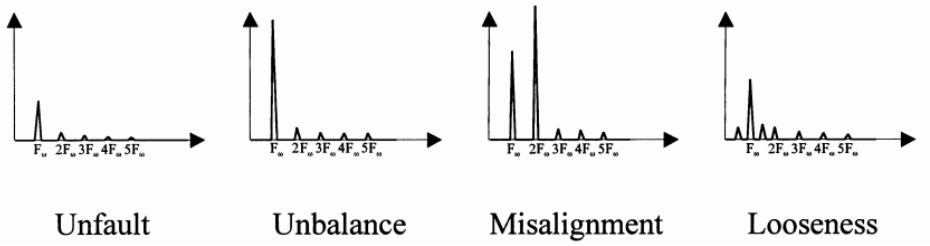

Figure 4.3: Spectrum of typical vibration faults of general rotating machinery elements. Source: [3]

4.3.2 Bearing defects

Bearing specific defects are faults at the inner and the outer race. The defect can be any imperfection on the surface of the race. When a ball of the bearing strikes a localized defect on of the race, it usually generates short high frequency resonance of the whole structure (bearing) [35]. This resonance then repeats at the BPFO or BPFI frequency, depending on which race the defect is.

4.3.3 Gear defects

A common defect of a gear is a broken or a worn tooth. A gear with such defect usually emits high amplitude vibrations and acoustic noise of frequency equal to GMF and its harmonics and subharmonics when it meshes with another toothed part of machinery. In other words, a gear with a damaged tooth emits vibration and acoustic signal at GMF whose amplitude is modulated[6] by the driving frequency.

4.3.4 Turbine defects

A turbine blade assembly can suffer from various defects which are often caused by imperfect manufacturing process such as improper joints of blades within the assembly. The defects on a blade of the turbine then typically cause the turbine to be unbalanced.

[6] Amplitude modulation is change of amplitude in time while keeping the same frequency of the oscillations.

Chapter 5

Experiments

This chapter describes experiments conducted upon real-world datasets. The goal of the experiments is to demonstrate the application of Fourier and Wavelet transforms in vibration and acoustic analysis of machinery. Our focus is revealing a defective condition of rotating machinery. For that purpose, we chose four publicly available datasets containing measurements of both defective and healthy machinery of the same type. The datasets contain vibration data only. However, based on characteristics of the data described in Chapter 4, acoustic emission should closely correlate with vibrations. Therefore we assume the vibration measurements to be enough for the demonstration.

Each experiment is done upon one dataset and consists of a description of the measurements in the dataset followed by analysis of the healthy and defective state. The analysis consists of processing the signals by DFT, DWT and CWT. We will not use STFT, since DWT and CWT should provide better time-frequency representation, as explained in the Chapter 3.

From DFT, we show the amplitude frequency spectrum. In order to achieve the best results of DFT and minimize spectral leakage, the input for DFT is always the entire measurement (typically several seconds) multiplied by Hanning window.

Since the output of both DWT and CWT is time localized, it would not be feasible to analyze scalograms obtained from the entire measurement. Moreover, it is not even necessary. Majority of the defects occur at frequencies equal to or higher than the driving frequency. Therefore, the length of input for DWT and CWT is always equal to several rotation cycles. We first show scalogram of DWT up to the maximum decomposition level. If DWT reveals high presence of a certain range of frequencies, CWT is then computed for the same input and the corresponding range of scales is sampled at finer resolution in order to provide more details. In the scalograms, the individual rotation cycles are separated by a vertical dashed line. The mother wavelets chosen for the transforms are Haar wavelet for DWT and real-valued Morlet wavelet for CWT.

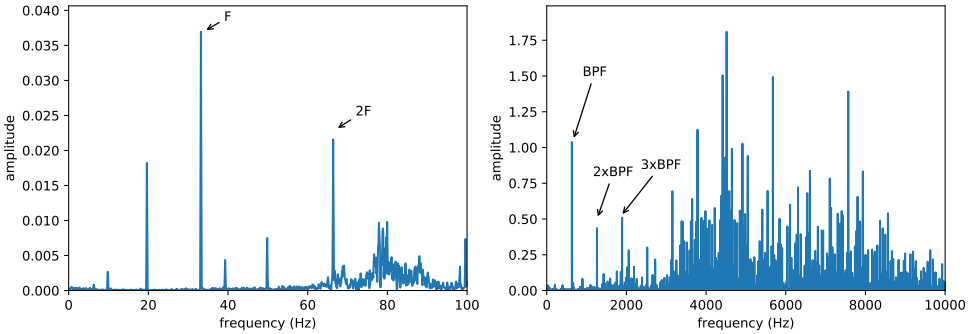

Figure 5.1: Frequecy spectra of the healthy turbine

The individual experiments are described in Sections 5.1-5.3. The summary of the experiments and the conclusion how or whether the methods revealed the defective state is then given in section 5.4.

Since the purpose of the experiments is purely demonstrative, we chose implementation in Python where many packages with Fourier and Wavelet transforms are available. NumPy [36] was used for computation of Discrete Fourier transform and PyWavelets [37] were used for computation of Continous and Discrete Wavelet transforms. The visualizations were made in Matplotlib [38]. Each experiment is written as a Jupyter Notebook [39] which allows us to easily reran the experiments.

5.1 Gas Turbine Dataset

Gas Turbine dataset contains two vibration measurements of a simplified turbine test rig. The data were measured by Gareth L. Forbes and were used, along with pressure measurements, to estimate turbine blade natural frequencies [40].

The turbine was equipped with 19 blades arrangement and ran at constant speed of 2000 rpm. During the first measurement, the turbine was in a healthy state while during the second measurement one blade was replaced by a shorter blade to simulate mass unbalance. Both measurements were taken at sampling rate 65336Hz and their length is 10 seconds each.

The driving frequency F is 33Hz. The blade pass frequency of the turbine is 632Hz.

5.1.1 Analysis of Healthy Turbine

Figure 5.1 shows the frequency spectrums of the healthy turbine at frequencies $[0, 100]$ and $[0, 10000]$. We are able to identify the blade pass frequency (BPF) with its first two harmonics and the driving frequency F and its first harmonic.

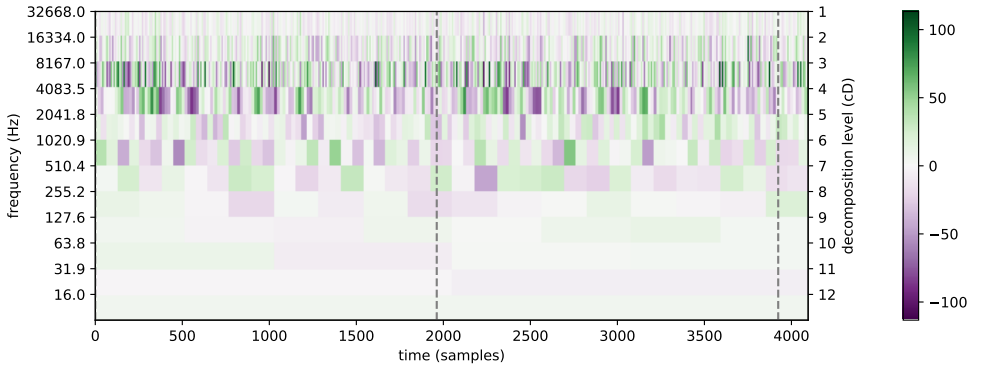

Figure 5.2: DWT scalogram of the healthy turbine

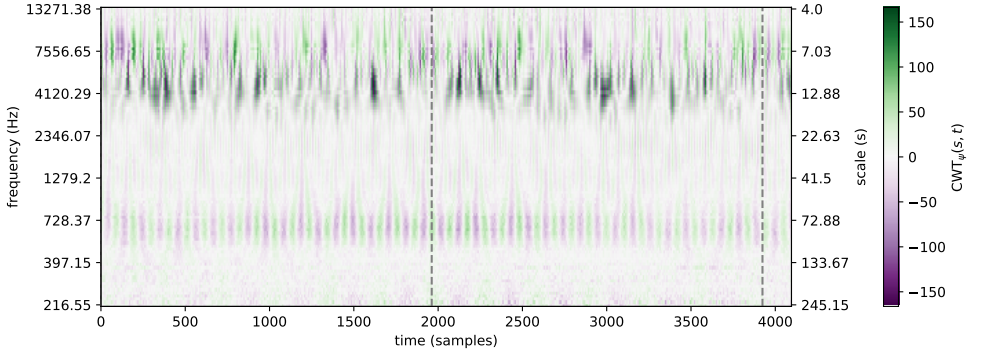

Figure 5.3: CWT scalogram of the healthy turbine

In the higher frequencies, there is a high presence of frequencies between 3000 and 9000Hz, especially around 4500Hz.

Figure 5.2 shows the scalogram obtained from DWT. As expected from the frequency spectra, we see high presence of frequency range $[2041, 8167]$ and $[510, 1020]$. Figure 5.3 shows the CWT scalogram where a periodic pattern of 19 times per rotation is visible around BPF. The higher frequencies around 4500Hz seem to follow similar periodicity as the BPF.

5.1.2 Analysis of Defect: Shorter Blade

Figure 5.4 shows the frequency spectrums of a turbine with one blade shorter which simulates mass unbalance defect. We see that the driving frequency is around two and a half times higher than at the basline data (0.36 compared to 0.14). The blade pass frequency is now lower by almost a half, but there is a high amplitude peak around frequency $3900Hz$. We can again see a visible distance between this frequency and other frequencies with high amplitude again of length equal to BPF.

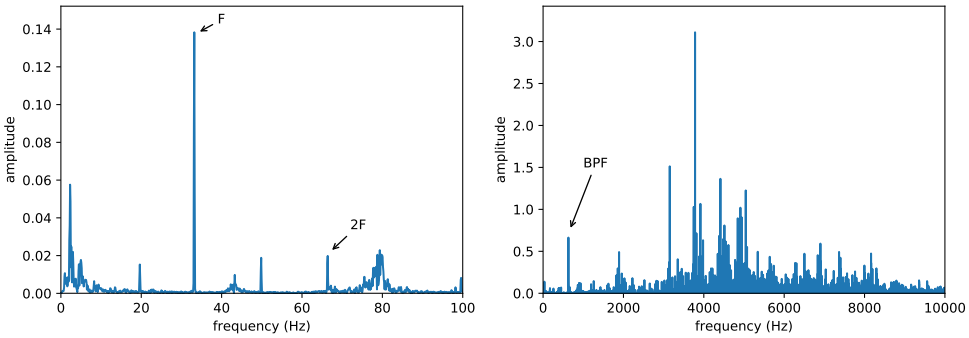

Figure 5.4: Frequecy spectrum of the turbine with one blade shorter

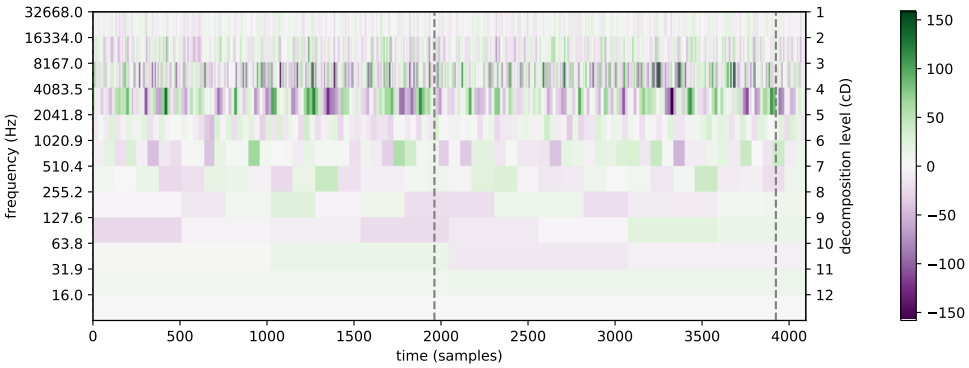

Figure 5.5: DWT scalogram of the turbine with one blade shorter

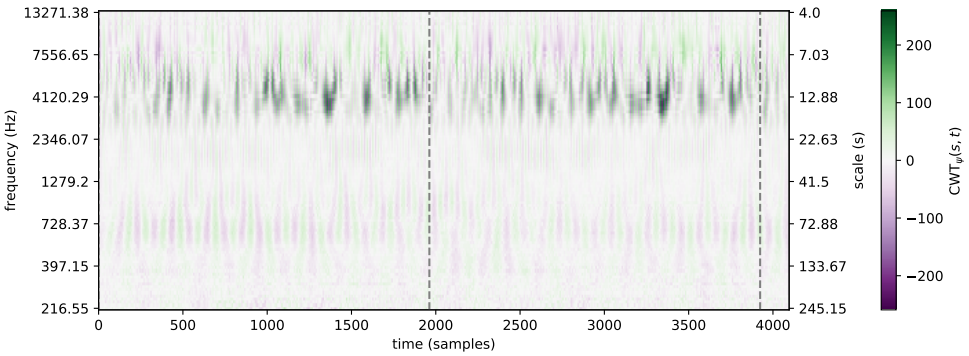

Figure 5.6: CWT scalogram of the turbine with one blade shorter

Figure 5.7: A fault found on the wind turbine gear, source: [4]

DWT scalogram in Figure 5.6 shows a little increase the presence of range where the driving frequency is. Aside that, it shows, similarly as DFT, significantly higher presence of frequencies at range $[2041, 8167]$ compared to rest of the frequencies. In the CWT scalogram, shown in Figure 5.6, we can identify a high presence of frequencies around 4000Hz with high coefficients repeating around 19 times per rotation (BPF).

5.2 High Speed Gear Dataset

High speed gear dataset was obtained from Acoustic and Vibration Database [4]. It consists of three radial vibration measurements taken on three different 3MW turbine gears of the same type. The measurement of the first turbine showed high initial vibrations and the turbine was stopped after one week of operation. A defect on a tooth of the gear was later found. The photo of the defect is shown in the Figure 5.7. The two other measurements were taken on gears of the same type with no known faults. For our experiment, we took one of the measurements taken on gear with no known faults as the baseline data.

The measurements were taken by an accelerometer with sampling rate 97969Hz and are 6 seconds long each. The gear had 32 teeth and ran at nominal speed 1800 rpm. The driving frequency is then 30 Hz and GMF is 960 Hz.

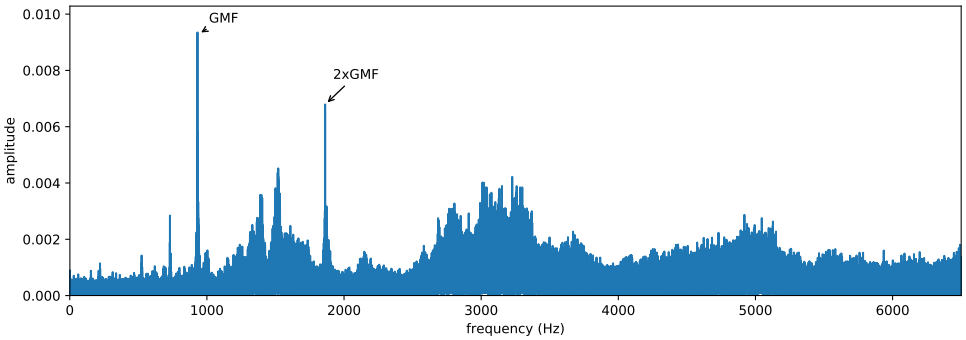

Figure 5.8: Frequency spectrum of a healthy gear

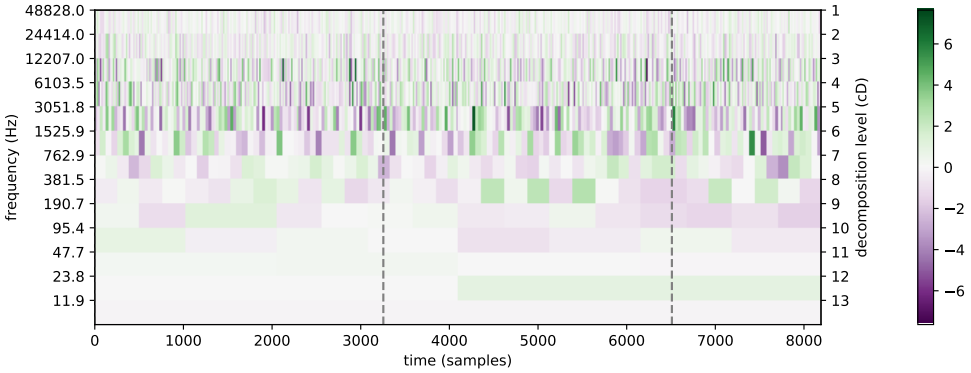

Figure 5.9: DWT scalogram of a healthy gear

5.2.1 Analysis of Healthy Gear

Figure 5.8 shows the frequency spectrum of the baseline data up to frequency 6500Hz. We can clearly identify GMF and its first harmonic 2xGMF.

DWT scalogram is shown in the Figure 5.9. We can see higher presence of frequencies at range $[762, 12207]$. CWT scalogram for the corresponding range is shown in the Figure 5.10.

5.2.2 Analysis of Defect: Damaged Tooth

Figure 5.11 shows the frequency spectrum of the gear with a damaged tooth. We can identify GMF and its first harmonic and subharmonic. Moreover, there are visible frequency sidebands around those frequencies with distance equal to the driving frequency.

Figure 5.12 shows a DWT scalogram. We see a pattern recurring once per rotation in the frequency range $[762, 3051]$. CWT scalogram shown in 5.13 then reveals the pattern in more detail. At the first harmonic and subharmonic

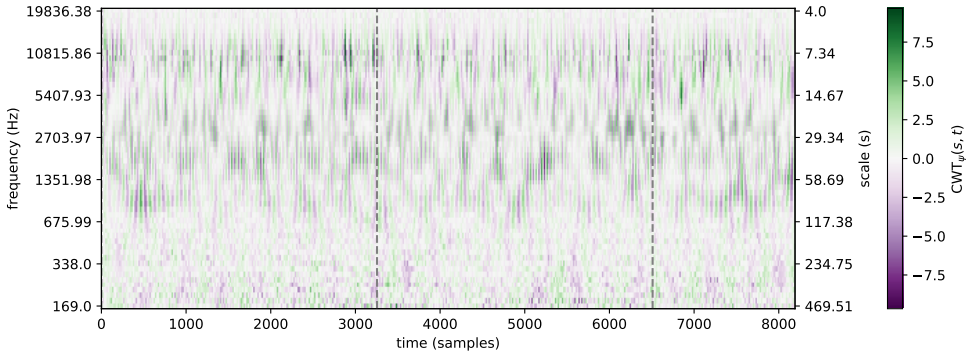

Figure 5.10: CWT scalogram of a healthy gear

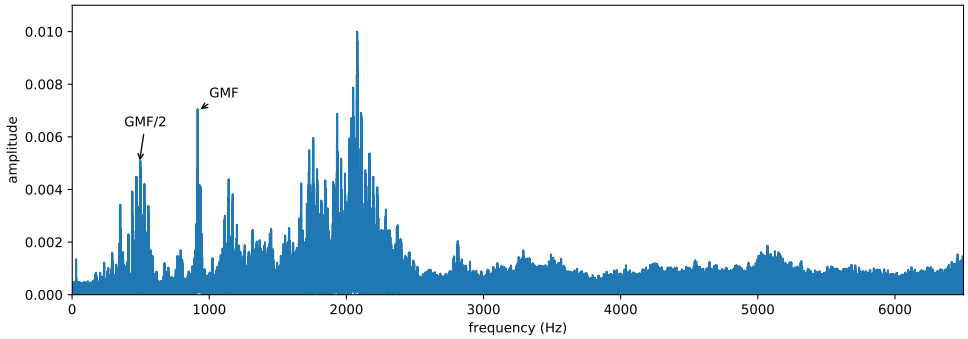

Figure 5.11: Frequency spectrum of the pinion with a damaged tooth

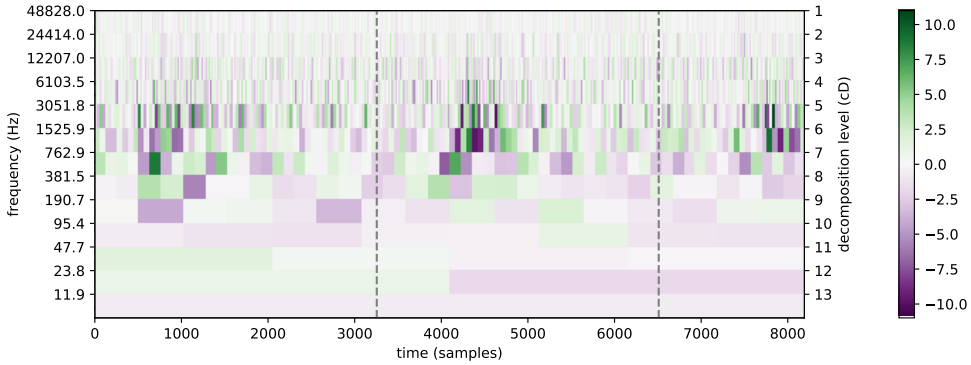

Figure 5.12: DWT scalogram of the pinion with a damaged tooth

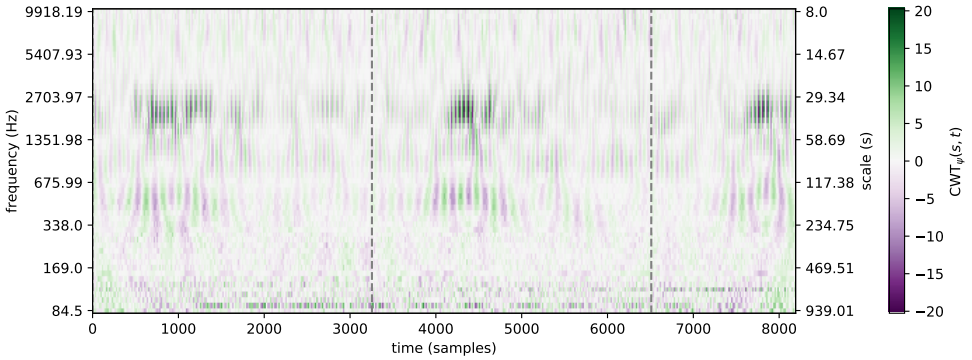

Figure 5.13: CWT scalogram of the pinion with a damaged tooth

of GMF, we can identify the moments when the damaged tooth of a pinion meshes with the teeth of the other gear.

5.3 Case Western Bearing Dataset

Case Western bearing dataset contains vibration measurement of ball bearings at different conditions. Specifically, it contains measurements of healthy bearings and bearings with seeded faults of different severity including inner race fault, outer race fault and ball fault. Each measurement contains description about the parameters of the fault (diameter and depth). The data were measured by Case Western Bearing Data Centre[7].

For purpose of our experiment, we chose the measurement of a healthy bearing and a bearing with an outer raceway fault of diameter 0.18mm and depth 0.28mm. For comparison, the outside diameter of the bearing is 5.2cm and the inside diameter is 2.5cm. During both measurements the bearing ran at constant speed of 1730 rpm. The characteristic frequencies of the bearing are:

- F = 1730/60 ≈ 28.8Hz
- Ball pass frequency outer race (BPFO) = 3.5848xF ≈ 103Hz
- Ball pass frequency inner race (BPFI) = 5.4152xF ≈ 156HZ
- Ball spin frequency (BSF) = 4.7135xF ≈ 136HZ

The measurements were taken by an accelerometer with of sampling rate 48000Hz and are 10 seconds long each.

[7]http://csegroups.case.edu/bearingdatacenter/pages/welcome-case-western-reserve-university-bearing-data-center-website

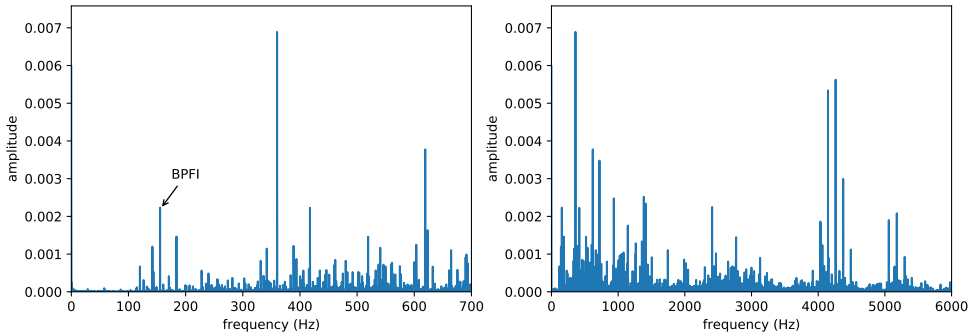

Figure 5.14: Frequency spectrum of a healthy bearing

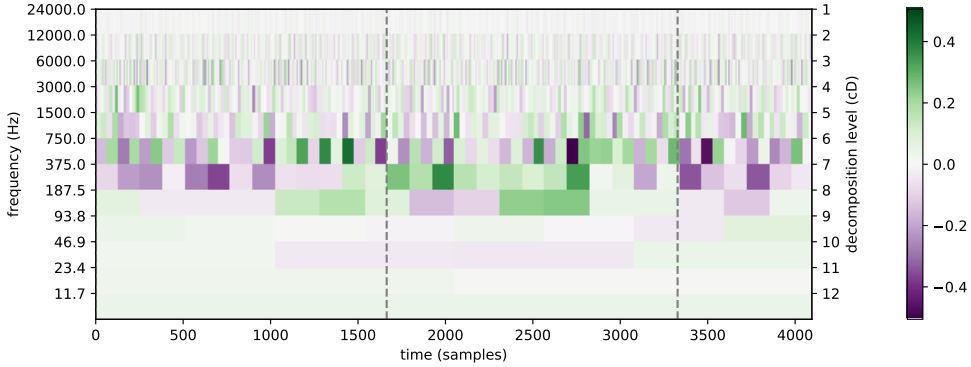

Figure 5.15: DWT scalogram of a healthy bearing

5.3.1 Analysis of Healthy Bearing

Figure 5.14 shows a frequency spectrum of a healthy bearing. We can identify BPFI. Aside that, the frequency around 360Hz ha high amplitude as well as some high frequencies above 4000Hz. However, it is not clear how to interpret their presence.

Figure 5.15 shows DWT scalogram which reveals that there is a pattern in the frequency range $[3000, 6000]$ recurring approximately 3.5 times per revolution. That indicates that those high frequencies above 4000Hz could relate to BPFO since BPFO is 3.58 times the driving frequency. Moreover, we see a high presence of frequencies at range $[187, 750]$ with no obvious pattern. CWT scalogram shown in the Figure 5.16 reveals a periodicity of around 11 times per revolution at frequencies around 380Hz. Based on that, we can assume that the frequencies around 380Hz could relate to the first harmonic of BPFI.

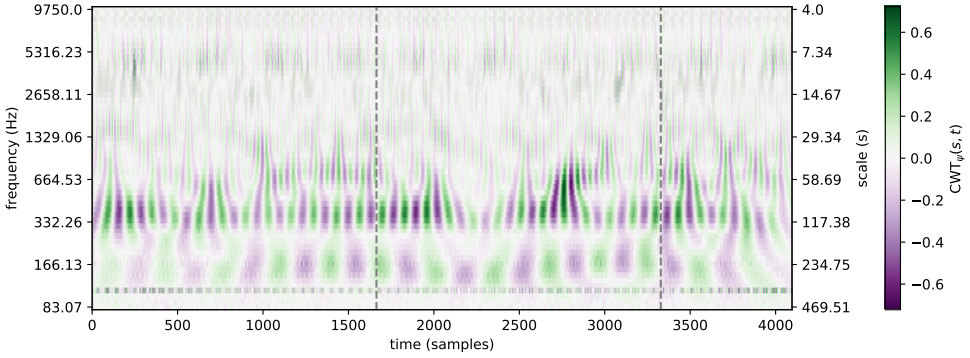

Figure 5.16: CWT scalogram of a healthy bearing

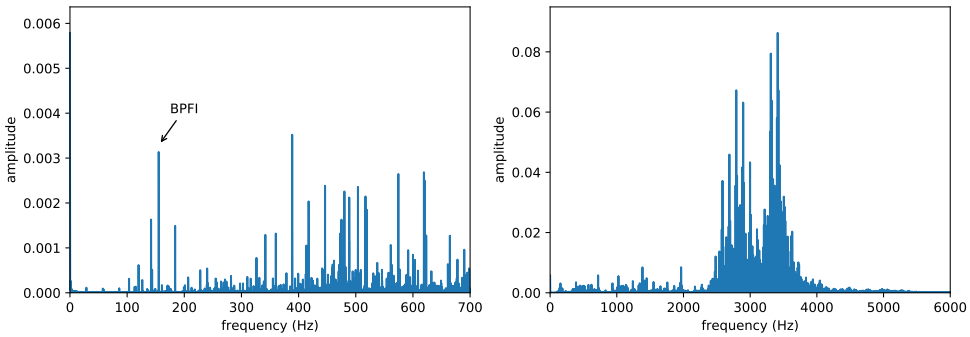

Figure 5.17: Frequency spectrum of a bearing with outer race fault

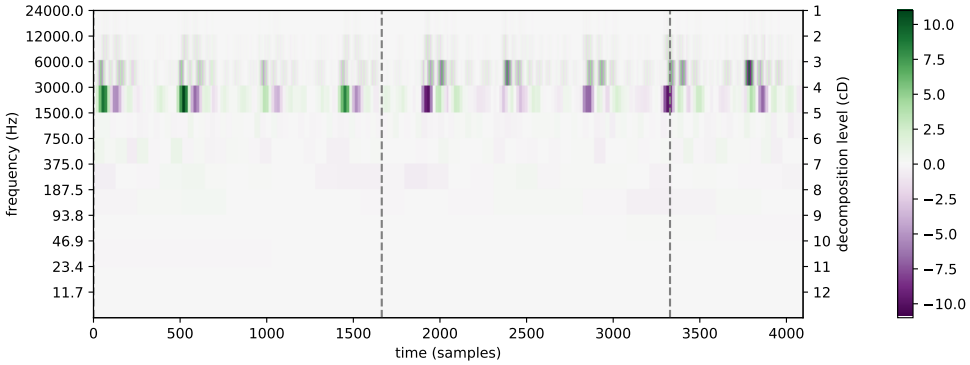

Figure 5.18: DWT scalogram of a bearing with an outer race fault

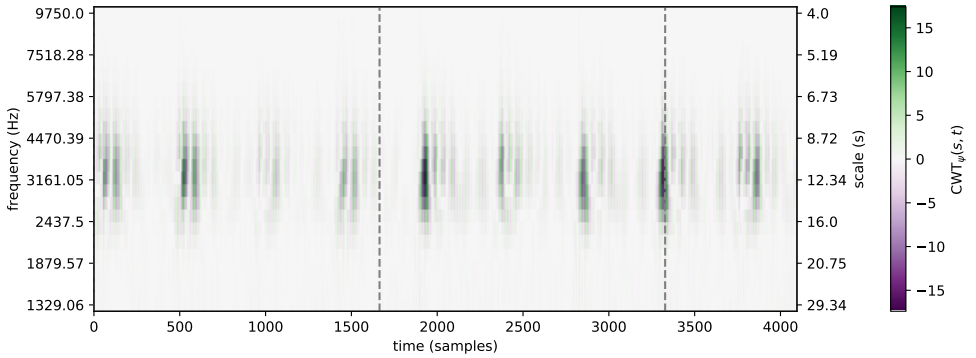

Figure 5.19: CWT scalogram of a bearing with an outer race fault

5.3.2 Analysis of Defect: Outer Race Fault

Figure 5.17 shows a frequency spectrum of a bearing with an outer race fault. We see the frequency spectrum for frequencies lower than 700Hz remains similar to the spectrum of a healthy bearing except the BPFI being now slightly higher. At the higher frequencies we see high rise of amplitudes at frequencies around 3000Hz. Howerer, it not clear how to interpret it.

DWT scalogram shown in figure 5.18 shows majority of energy of the signal being concentrated at frequency range from 1500 to 6000Hz. Moreover, there is a clear pattern of periodicity around 3.5 times per revolution which matches BPFO. Scalogram of CWT shown in figure 5.19 reveals that it corresponds to the frequencies around 3000Hz and shows exact moments when the ball strikes the defect at the outer race.

5.4 Results

The first experiment compared a turbine suffering from a mass unbalance with a healthy turbine. Fourier transform revealed that the frequency spectra of the two turbines differ in amplitude of the driving frequency – a turbine with mass unbalance had almost three times higher amplitude. The difference in the amplitude of the driving frequency was visible in the scalogram of the Wavelet transforms as well, but no additional information was revealed compared to Fourier transform.

The second experiment compared a gear suffering from a damaged tooth with a healthy gear. Fourier transform revealed that the frequency spectrum of the gear with damaged tooth differs from a healthy gear in the presence of frequency side bands around gear mesh frequency and its harmonics and subharmonics. From that, we could assume a presence of a fault at GMF. Wavelet transform then revealed a pattern recurring once per revolution of the gear which showed the specific vibration patterns generated when the

damaged tooth meshed with the other toothed part of machinery.

The third, and the last, experiment compared a bearing suffering from an outer race fault with a healthy bearing. Fourier transform revealed presence of high frequencies in the frequency spectrum of the bearing with the fault, but there was no clear connection between the characteristic frequencies and the fault. Both DWT and CWT then revealed that there are periodic patterns at those high frequencies whose periodicity matched with the characteristic frequencies of the bearing. When the bearing suffered from the outer race fault, the corresponding characteristic frequency matched the periodicity of the pattern at the high frequencies and exact moments when a ball striked the defect were visible.

From the results of the experiments, we conclude that both Fourier and Wavelet tranforms can reveal defective state of the machinery. Fourier transform can detect mass unbalance, as seen in the first experiment, by presence of higher amplitude of the driving frequency. It can also detect presence of faults at higher frequencies by frequency sidebands around characteristic frequencies of the machinery, as seen in the second experiment. However, in the third case, when the defect was characterized by short high frequency patterns, it struggled to identify type of the fault. Wavelet transforms were as well able to identify specific faults, as seen in the second and the third experiment, and moreover, they were able to localize the defective behaviour in time.

Chapter 6

Conclusion

In the first part of this Thesis, we described two state-of-the-art spectral analysis methods – Fourier and Wavelet transform. The description was provided with examples of signal analysis by those methods. In the second part, we focused on vibration and acoustic analysis of machinery. We described characteristics of vibration and acoustic signals emitted by the machinery and how those characteristics can be used to identify a condition of the machinery component using spectral analysis. Finally, the experiments conducted upon real world data verified that Fourier and Wavelet transforms can be applied for condition monitoring of the machinery by comparison of its spectrum with a spectrum of a healthy machinery.

In the experiments, we compared the spectrums manually – by eye. Therefore, future work could focus on automatization of this process possibly leading to early detection of the faults or their prediction based on historical data.

Bibliography

[1] Fernandez, A. Vibration analysis learning, Study of vibration. 2017. Available from: http://www.power-mi.com/content/study-vibration

[2] Felten, D. Understanding Bearing Vibration Frequencies. 2003. Available from: http://electromotores.com/PDF/InfoT%C3%A9cnica/EASA/Understanding%20Bearing%20Vibration%20Frequencies.pdf

[3] Betta, G.; Liguori, C.; et al. A DSP-based FFT-analyzer for the fault diagnosis of rotating machine based on vibration analysis. *IEEE Transactions on Instrumentation and Measurement*, volume 51, no. 6, Dec 2002: pp. 1316–1322, ISSN 0018-9456, doi:10.1109/TIM.2002.807987.

[4] Bechhoefer, E. High speed gear dataset. Available from: http://data-acoustics.com/measurements/gear-faults/gear-1/

[5] Ibrahim, R.; Watson, S. Advanced Algorithms for Wind Turbine Condition Monitoring and Fault Diagnosis. 9 2016. Available from: https://dspace.lboro.ac.uk/dspace-jspui/bitstream/2134/23234/1/369_WindEurope2016presentation.pdf

[6] Al-Badour, F.; Sunar, M.; et al. Vibration analysis of rotating machinery using time–frequency analysis and wavelet techniques. *Mechanical Systems and Signal Processing*, volume 25, no. 6, 2011: pp. 2083 – 2101, ISSN 0888-3270, doi:https://doi.org/10.1016/j.ymssp.2011.01.017, interdisciplinary Aspects of Vehicle Dynamics. Available from: http://www.sciencedirect.com/science/article/pii/S0888327011000276

[7] Vernekar, K.; Kumar, H.; et al. Gear Fault Detection Using Vibration Analysis and Continuous Wavelet Transform. *Procedia Materials Science*, volume 5, 2014: pp. 1846 – 1852, ISSN 2211-8128, doi:https://doi.org/10.1016/j.mspro.2014.07.492, international Conference on Advances in Manufacturing and Materials Engineering, ICAMME 2014.

Available from: http://www.sciencedirect.com/science/article/pii/S2211812814008578

[8] Bendjama, H.; Bouhouche, S.; et al. Application of Wavelet Transform for Fault Diagnosis in Rotating Machinery. volume 2, 01 2012: pp. 82–87.

[9] Li, H.; Zhang, Y.; et al. Application of Hermitian wavelet to crack fault detection in gearbox. *Mechanical Systems and Signal Processing*, volume 25, no. 4, 2011: pp. 1353 – 1363, ISSN 0888-3270, doi: https://doi.org/10.1016/j.ymssp.2010.11.008. Available from: http://www.sciencedirect.com/science/article/pii/S0888327010004115

[10] Douglas C. Montgomery, M. K., Cheryl L. Jennings. *Introduction to Time Series Analysis and Forecasting*. Wiley-Interscience, second edition, 2015, ISBN 978-1-118-74511-3.

[11] Rayner, J. Spectral Analysis. In *International Encyclopedia of the Social & Behavioral Sciences*, edited by N. J. Smelser; P. B. Baltes, Oxford: Pergamon, 2001, ISBN 978-0-08-043076-8, pp. 14861 – 14864, doi:https://doi.org/10.1016/B0-08-043076-7/02514-6. Available from: https://www.sciencedirect.com/science/article/pii/B0080430767025146

[12] Bremaud, P. *Mathematical Principles of Signal Processing: Fourier and Wavelet Analysis*. Springer New York, 2010.

[13] Morin, D. Fourier analysis. 2009. Available from: http://www.people.fas.harvard.edu/~djmorin/waves/Fourier.pdf

[14] Kalvoda, T.; Štampach, F. Vybrané matematické metody, BI-VMM. 2018. Available from: http://sagemath.fit.cvut.cz/deploy/bi-vmm/bi-vmm-prednaska.pdf

[15] Heideman, M.; Johnson, D.; et al. Gauss and the history of the fast fourier transform. *IEEE ASSP Magazine*, volume 1, no. 4, October 1984: pp. 14–21, ISSN 0740-7467, doi:10.1109/MASSP.1984.1162257.

[16] James W. Cooley, J. W. T. An Algorithm for the Machine Calculation of Complex Fourier Series. *Mathematics of Computation*, volume 19, no. 90, 1965: pp. 297–301.

[17] Cazelais, G. Linear Combination of Sine and Cosine. 2007. Available from: http://pages.pacificcoast.net/~cazelais/252/lc-trig.pdf

[18] Understanding FFTs and Windowing. Available from: http://download.ni.com/evaluation/pxi/Understanding%20FFTs%20and%20Windowing.pdf

[19] Stéphane, M. *A Wavelet Tour of Signal Processing (Third Edition)*. Boston: Academic Press, third edition edition, 2009, ISBN 978-0-12-374370-1, doi:https://doi.org/10.1016/B978-0-12-374370-1.50001-9. Available from: https://www.sciencedirect.com/science/article/pii/B9780123743701500000

[20] Daubechies, I. *Ten Lectures On Wavelets*, volume 93. 01 1992.

[21] Kaiser, G. *A friendly guide to wavelets*. Birkhäuser, 1994.

[22] Rao, R.; Bopardikar, A. *Wavelet Transforms: Introduction to Theory and Applications*. Pearson Education Asia, 1999, ISBN 9788178082516.

[23] Strang, G. Wavelets Transforms Versus Fourier transforms. volume 28, 05 1993.

[24] Guido, R. C. A note on a practical relationship between filter coefficients and scaling and wavelet functions of Discrete Wavelet Transforms. *Applied Mathematics Letters*, volume 24, no. 7, 2011: pp. 1257 – 1259, ISSN 0893-9659, doi:https://doi.org/10.1016/j.aml.2011.02.018. Available from: http://www.sciencedirect.com/science/article/pii/S0893965911000905

[25] Polikar, R. The Wavelet Tutorial. Available from: http://web.iitd.ac.in/~sumeet/WaveletTutorial.pdf

[26] Rioul, O.; Vetterli, M. Wavelets and signal processing. volume 8, 10 1991: pp. 14 – 38.

[27] Scale to frequency - MATLAB scal2frq. Available from: https://www.mathworks.com/help/wavelet/ref/scal2frq.html

[28] Gomez-Luna, E.; Aponte, G.; et al. Application of Wavelet Transform to Obtain the Frequency Response of a Transformer From Transient Signals—Part II: Practical Assessment and Validation. volume 29, 10 2014: pp. 2231–2238.

[29] Continuous and Discrete Wavelet Transforms - MATLAB & Simulink. Available from: https://www.mathworks.com/help/wavelet/gs/continuous-and-discrete-wavelet-transforms.html

[30] Continuous 1-D wavelet transform - MATLAB cwt. Available from: https://www.mathworks.com/help/wavelet/ref/cwt.html

[31] Haar, A. Zur Theorie der orthogonalen Funktionensysteme. *Mathematische Annalen*, volume 69, no. 3, 1910: pp. 331–371.

[32] Daubechies, I. Orthonormal bases of compactly supported wavelets. *Communications on Pure and Applied Mathematics*, volume 41, no. 7: pp. 909–996, doi:10.1002/cpa.3160410705, https://onlinelibrary.wiley.com/doi/pdf/10.1002/cpa.3160410705. Available from: https://onlinelibrary.wiley.com/doi/abs/10.1002/cpa.3160410705

[33] Mallat, S. G. A theory for multiresolution signal decomposition: the wavelet representation. *IEEE Transactions on Pattern Analysis and Machine Intelligence*, volume 11, no. 7, Jul 1989: pp. 674–693, ISSN 0162-8828, doi:10.1109/34.192463.

[34] A. Shirude, S. Y. G. A Review on Vibration Analysis for Misalignment of Shaft in Rotary Systems by Using Discrete Wavelet Transform. *IJRME - Internaltional Journal of Research in Mechanical Engineering*, volume 3, 2016, ISSN 2349-3860. Available from: https://pdfs.semanticscholar.org/59d3/ae01472713003c6698f099f5843c1fa8ac4e.pdf

[35] Li, H.; Fu, L.; et al. Bearing fault diagnosis based on amplitude and phase map of Hermitian wavelet transform. volume 25, 11 2011: pp. 2731–2740.

[36] Travis E, O. *A guide to NumPy*. USA: Tregol Publishing, 2006.

[37] Lee, G.; Wasilewski, F.; et al. PyWavelets - Wavelet Transforms in Python. 2006-, [Online; accessed 2018-05-02]. Available from: https://github.com/PyWavelets/pywt

[38] development team, T. M. Matplotlib: Python plotting — Matplotlib 2.2.2. Available from: https://matplotlib.org

[39] Kluyver, T.; Ragan-Kelley, B.; et al. Jupyter Notebooks – a publishing format for reproducible computational workflows. 01 2016.

[40] Forbes, G. L.; Randall, R. B. Estimation of turbine blade natural frequencies from casing pressure and vibration measurements. *Mechanical Systems and Signal Processing*, volume 36, no. 2, 2013: pp. 549 – 561, ISSN 0888-3270, doi:https://doi.org/10.1016/j.ymssp.2012.11.006. Available from: http://www.sciencedirect.com/science/article/pii/S0888327012004645

Appendix A

Mathematical symbols

$\mathbb{N}$	domain of natural numbers
$\mathbb{R}$	domain of real numbers
$\mathbb{R}^+$	domain of positive real numbers
$\mathbb{C}$	domain of complex numbers
$\Re(c)$	real part of the complex number c
$\Im(c)$	imaginary part of the complex number c
$\sum_k$	sum over all values k for which is the expression in the sum defined

Appendix B

Acronyms

BPF Blade pass frequency

BPFO Ball pass frequency outer race

BPFI Ball pass frequency inner race

BSF Ball spin frequency

CFT Continuous Fourier transform

CPF Cage pass frequency

CWT Continuous Wavelet transform

DFT Discrete Fourier transform

DWT Discrete Wavelet transform

FFT Fast Fourier transform

FT Fourier transform

GMF Gear mesh frequency

STFT Short-time Fourier transform

WT Wavelet transform

Appendix C

Contents of enclosed CD

```
experiments ..... experiments in Jupyter Notebooks
data ..... data for experiments
thesis ..... LaTeX source codes and PDF of the thesis
```